https://ntrs.nasa.gov/search.jsp?R=19890013243 2020-03-20T02:28:13+00:00Z

NASA Technical Memorandum 4114

Hardware and Operating Features of the Adaptive Wall Test Section for the Langley 0.3-Meter Transonic Cryogenic Tunnel

Raymond E. Mineck
Langley Research Center
Hampton, Virginia

National Aeronautics and
Space Administration
Office of Management
Scientific and Technical
Information Division

1989

Summary

A 13- by 13-inch adaptive wall test section has been installed in the Langley 0.3-Meter Transonic Cryogenic Tunnel circuit. This new test section has four solid walls and is configured for two-dimensional airfoil testing. The top and bottom walls are flexible and movable, whereas the sidewalls are rigid and fixed. The test section has a turntable to support airfoil models, a survey mechanism to probe the model wake, and provisions for a sidewall boundary-layer-control system. Details of the adaptive wall test section, the tunnel circuit modifications, the supporting instrumentation, the monitoring and control hardware, and the wall adaptation strategy are discussed. Shakedown tests with the test section empty covered a Mach number range from 0.2 to 0.9 and a Reynolds number range from 10×10^6 to 100×10^6/foot. Shakedown tests with airfoil models having chords from 6.0 to 13.0 inches covered a Mach number range from 0.3 to 0.8 and a chord Reynolds number range from 3×10^6 to 72×10^6. Sample results of shakedown tests with the test section empty and with a typical airfoil installed are also included.

Introduction

The artificial constraint of wind-tunnel test section walls on the flow field can introduce errors in the simulation of "free air" conditions. Corrections for wall-induced interference in the test section can be applied to wind-tunnel test data after the test. (See ref. 1.) In extreme cases, the wall interference can become so severe that the test data cannot be corrected to equivalent free air conditions. An alternative approach to correcting the data after the test is to reduce or eliminate the interference at its source during the test. This approach is called the adaptive wall test section concept in this paper. Modern adaptive wall test sections were put on a sound technical footing by Sears in reference 2. He demonstrated that wall interference would be eliminated if two independent flow-field parameters are matched on a control surface. This can be accomplished in different ways as shown by the different configurations of adaptive wall test sections which are described in reference 3. The flow field at the control surface can be modified to match the desired parameters by varying the wall porosity, the pressure behind a porous wall, or the shape of a solid wall. Each of these concepts has its strengths and weaknesses.

Based on the work at the University of Southampton in England (ref. 4), a solid adaptive wall test section was built and installed in the Langley 0.3-Meter Transonic Cryogenic Tunnel (0.3-m TCT) circuit in 1985. This report presents details of the adaptive wall test section, the tunnel circuit modifications, the supporting instrumentation, the monitoring and control hardware, and the wall adaptation strategy. Samples of the results from the shakedown tests with the test section empty and with a typical airfoil model installed are also included.

Symbols

A	cross-sectional area, feet^2
B.L.	boundary layer
BLC	boundary-layer control
C_p	local pressure coefficient
CRT	cathode-ray tube
c	airfoil model chord, inches
c_d	section drag coefficient
c_m	section pitching-moment coefficient
c_n	section normal-force coefficient
GN_2	gaseous nitrogen
h	distance to describe internal contour of first contraction section, inches
LED	light-emitting-diode display
LN_2	liquid nitrogen
LVDT	linear variable differential transformer
M	local Mach number
$\bar{p}$	average static pressure, pounds per inch^2
R	Reynolds number per foot
r	distance to describe internal contour of first contraction section, inches
sta.	station measured from center of turntable, positive downstream, inches
TCT	transonic cryogenic tunnel
t_f	thickness of flexure in wall rib, inches
t_p	thickness of wall attachment plate, inches
t_w	thickness of flexible wall, inches

w	distance to describe internal contour of second contraction section, inches
x	distance measured from center of turntable, positive downstream, inches; chordwise position on airfoil, inches
y	distance to describe internal contour of second contraction section, inches
z	displacement of flexible wall, positive up, inches
α	angle of attack, degrees
Δp	deviation of pressure from average static pressure, pounds per inch^2
η	lateral position nondimensionalized by test section semiwidth

Langley 0.3-Meter Transonic Cryogenic Tunnel

The 0.3-m TCT is a fan driven, cryogenic pressure tunnel which uses nitrogen (GN_2) as a test gas. It is capable of operating at stagnation temperatures from 327 K to about 80 K and at stagnation pressures from 1.2 to 6.0 atmospheres. The fan speed is continuously variable so that the free-stream Mach number can be varied from about 0.2 to 0.9. From 1976 until 1985, the 0.3-m TCT was frequently used to study airfoil aerodynamic characteristics at high Reynolds numbers. The tunnel had an 8- by 24-inch test section with slotted top and bottom walls. A sketch showing the tunnel circuit with this test section is presented at the top of figure 1. Details of the development of the 0.3-m TCT and the slotted test section may be found in reference 5.

An adaptive wall test section, also configured for two-dimensional airfoil testing, was designed and built for the 0.3-m TCT. The design was based on the test section of reference 4. The adaptive wall test section replaced the 8- by 24-inch slotted test section in 1985. During the installation of the new test section, modifications to the tunnel circuit were completed to improve the tunnel operating characteristics. A new contraction section was installed to match the square cross section of the new adaptive wall test section. A longer, high-speed diffuser was installed to avoid the separation in that part of the tunnel circuit. Spacers (short, straight sections) were placed downstream of the screens and downstream of the test section to provide space for a future high-contraction-ratio entrance cone and for a future three-dimensional model sting-support system. A sketch of the tunnel circuit with the adaptive wall test section and the tunnel circuit modifications shaded is presented at the bottom of figure 1. The various components of the tunnel with the 13- by 13-inch adaptive wall test section installed are identified in figure 2. A photograph of the upper leg of the tunnel circuit is presented in figure 3. Details of the adaptive wall test section, the new contraction cone, and the new high-speed diffuser are presented in the following sections.

Adaptive Wall Test Section

The layout of the adaptive wall test section with the left plenum wall removed is presented in figure 4. A photograph of the interior of the plenum is shown in figure 5. All structural components of the test section shell and the fixed sidewalls are aluminum. The test section is configured for two-dimensional airfoil testing with the model suspended between two turntables. The angle-of-attack drive system, located outside the plenum, rotates the turntables. A total-pressure rake traverses vertically at one of three positions downstream of the model.

Details of the plenum side of the test section are presented in figure 6. The test section has four solid walls and is 13 inches square at the entrance. The top and bottom walls are flexible and movable, whereas the sidewalls are rigid and fixed with no divergence. The flexible walls are made from stainless steel and are 71.70 inches long. Upstream, each flexible wall is bolted to the forward bulkhead of the test section; downstream, each is held in place by a sliding joint in the rear bulkhead. The angle of the sliding joint matches the divergence angle of the high-speed diffuser. Twenty-one jacks, numbered consecutively from upstream to downstream, control the position of each flexible wall. The first jack on the top flexible wall is number 1 and the first jack on the bottom flexible wall is number 22. The jack stations are given in figure 7. The flexible walls define two flow regions. The forward region from station -29.75 to 25.05 defines the test section. Eighteen jacks control the shape of the test section and are nonuniformly spaced to provide finer control of the wall shape near the model. Wall thickness is reduced near the model (between stations -8.00 and 19.25) where the bending is greatest. (See fig. 7.) The rearward region defines a variable geometry diffuser between the test section exit (station 25.05) and the fixed-angle, high-speed diffuser (station 49.05). Here, the flexible walls are bent outward 4.1° to merge with the entrance of the high-speed diffuser which

is 15.36 inches high. Three jacks control the shape of the variable geometry diffuser.

The flexible walls are 12.94 inches wide to prevent binding with the sidewalls which are located 13.00 inches apart. Seals are provided between the edges of the flexible top and bottom walls and the fixed sidewalls to prevent flow from leaking from the test section into the plenum. The original design, shown in figure 8(a), used 0.25-inch-thick felt with the side facing the sidewall beveled to a point. The felt was attached to the nonflow side of the flexible wall with spring clips. As the flexible wall moved up and down, the felt would work into the gap causing binding between the flexible wall and the sidewall. This movement of the felt led to large increases in jack loads and motor stalling. The felt has been replaced with DuPont Teflon tubing held in place with a spring-like bracket as shown in figure 8. This arrangement has proved satisfactory.

A sketch of the wall positioning hardware is presented in figure 9 and a photograph is presented in figure 10. Each jack is driven by a stepping motor. Stepping motors were chosen to provide position control by using a digital computer. This type of motor is also resistant to burnout when stalled. Each stepping motor drives a 90°, 10:1 reduction gearbox which turns a jackscrew to raise or lower a crosshead. Two drive rods, pinned to each crosshead, penetrate the pressure shell through a seal. The linear motion of the drive rod simplifies the seal design. The hole in each drive rod for the pin is elongated laterally to allow the distance between the drive rods to change as the pressure shell expands and contracts with temperature. A "flexible" attachment plate, made from beryllium-copper alloy, is connected to the drive rods. The plate thickness was selected to prevent buckling of the plate with a differential pressure of 8 psi across the flexible wall. The plate is attached to the flexible wall through a flexure in the rib on the nonflow side of the wall. The plate thickness and flexure size are presented in figure 7. Each flexible plate is rigidly attached to both the drive rods and to the nonflow side of the flexible wall. These rigid attachments lead to two problems: a local wall waviness and increased jack loads. The upper end of the flexible attachment plate is kept vertical by the attachment to the drive rods. As the wall deflects, the local normal to the flexible wall is no longer vertical causing a moment at the lower attachment point. Such moments reduce the local wall slope which leads to a waviness in the flexible wall shape between the jack stations. As the wall deflects, the attachment point on the back side of the flexible wall moves upstream. This longitudinal displacement forces the flexible attachment plate to bend and put increased side loads on the drive rod seals. These increased side loads put larger loads on the stepping motors. The side loads as well as the local waviness in the flexible wall can be reduced if the rigid attachments at both ends of the flexible plate are replaced with pinned joints. Pinned joints allow for longitudinal displacement and eliminate the moment at the attachment to the flexible wall.

Linear variable differential transformers (LVDT's) are used to measure the jack movement directly and the wall displacement indirectly. They are mounted to the frame which supports the stepping motors as shown in figure 9. The movable core of each LVDT is attached to the crosshead which is assumed to vary directly with the wall position. The design displacement of each jack is from 1 inch down to 3 inches up; however, the current wall attachment method prevents these displacements from being reached. All wall positioning system drive components are located outside the cryogenic environment to simplify access and to eliminate the problems associated with thermal isolation.

A photograph of the test section viewed through the opening for one of the turntables is presented in figure 11. The model is installed between the two turntables in the model mounting plates. The turntables are 15 inches in diameter and the model mounting plates can accommodate models with chords up to 13 inches. Optical quality quartz glass can be installed in the viewing port above the model for a limited flow visualization capability. A photograph of an airfoil model in the model mounting plates ready for installation is shown in figure 12(a). The same model after installation is shown in figure 12(b). Note the angle-of-attack drive rod to rotate the turntables and the angle-of-attack encoder used to measure the angular position of the turntable. The angle-of-attack drive has a range of 40°. The angle-of-attack drive motor, located above the test section, is controlled by the computer directing the acquisition of the research data.

The test section layout in figure 4 shows a rake drive system which translates the wake rake support block. The support block has provisions for mounting a wake rake at one of three stations: 12.50, 17.50, or 22.50 on the left sidewall. The sketch of the wake rake is presented in figure 13. A photograph of the wake rake installed in the center position is presented in figure 14. The rake has six total-pressure probes and three static-pressure probes. The total-pressure probes are located at $\eta = 0$ (centerline), -0.212, -0.318, -0.529, -0.635, and -0.847. The static-pressure probes are located at $\eta = -0.106$, -0.423, and -0.741. The tips of the probes are 1.55 inches upstream of the center of the mounting stations in the support block. The probe tips are at station 10.95 for

the forward position, at station 15.95 for the center position, and at station 20.95 for the rear position. Three columns of static-pressure orifices are located on the right sidewall roughly opposite the three possible probe tip locations: stations 10.75, 15.75, and 20.75. The eight orifices in each column are located at ±4.00, ±3.00, ±2.00, and ±1.00 inches from the centerline. Either the pressures from the column of orifices on the right sidewall or the pressures from the static-pressure probes on the wake rake can be used to determine the wake static pressure. The rake traversing limits are 5 inches up and 3 inches down. The rake drive motor, located above the test section, is controlled by the computer directing the acquisition of research data.

A sidewall boundary-layer-control (BLC) system may be used with the adaptive wall test section. The system was retained from the previous 8- by 24-inch slotted test section. Details of the BLC system with the previous test section may be found in reference 6. Ductwork connects the back side of a thin porous plate to the BLC system. Pressures below the test section static pressure are applied to the nonflow side of the plate to thin the sidewall boundary layer. A flow control valve is located in each duct so that separate control of the removal rate from each side is possible. The system operates in either an active or a passive mode. In the passive mode, the back side of porous plates is vented to the atmosphere through a flow control valve. The mass removal is limited by the difference between the test section static pressure and the atmospheric pressure. In the active mode, a compressor is connected to the back side of the porous plates. The compressor exhaust is injected back into the tunnel circuit downstream of the test section as shown in figure 2. The mass removal is limited by the compressor capability. Each porous plate measures 14 by 7 inches and is centered 14.25 inches upstream of the center of the turntable. (See fig. 6.) The porous plates have a sandwich construction. The side exposed to the tunnel flow is a thin plate with electron-beam-drilled holes. The surfaces of the plates are etched and polished to obtain a smooth flow surface. A honeycomb and a heavy perforated plate are bonded to the thin plate to provide stiffness. This fabrication technique prevents any appreciable thickening of the boundary layer due to the perforations.

Modified Contraction Section

The contraction cone for the adaptive wall test section is split into two pieces as shown in figures 1 and 15. A short spacer was placed between the screen section and the first contraction piece. The screen section, located just upstream of the spacer and the contraction sections, is 48 inches in diameter. Three 40-mesh (per inch) screens made with 0.0065-inch-diameter wire are used. The contraction ratio is 10.7:1 based on the nominal 13- by 13-inch cross section of the test section. Eight instrument mounting blocks are available for installing the probes to measure the total temperature and the total pressure at station −105.53.

The upstream or first contraction piece from the 8- by 24-inch test section was retained with the new adaptive wall test section. Details of this piece are shown in figure 16. The upstream part changes the cross section from circular to a 16-sided polygon. The downstream part blends the 16-sided polygon into an 8-sided polygon.

A new downstream or second contraction piece was built for the adaptive wall test section. This piece, shown in figure 17, blends the 8-sided polygon (octagon) from the first contraction piece into the square of the test section inlet.

Modified High-Speed Diffuser

The new high-speed diffuser consists of three pieces as shown in figure 1. The first section is 24 inches long and changes the cross section from a rectangle to a circle. This transition piece, sketched in figure 18, provides a nearly constant cross-sectional area distribution. The second section is 60 inches long with a circular cross section and a divergence cone half-angle of 1.2°. The third section is 110.5 inches long with a circular cross section and a cone half-angle of 3.0°. The small diffuser angles in the second and third pieces will help keep the flow attached for the expected test conditions. The GN_2 removed by the BLC system may be reinjected at four places in the third section as shown in figure 1.

Instrumentation

Jack position is sensed at each crosshead with an LVDT with a design displacement of 6 inches. The calibration of a typical LVDT is presented in figure 19. The LVDT output voltage is nonlinear with displacement near the ends of its travel. These data are excluded from the linear, least-squares curve fit indicated by the solid line. Only the slope from the curve fit of the transformer is used. The offset is determined when the LVDT is installed by setting the jack to zero displacement and recording the transformer output. LVDT installation procedures ensured that the linear output range coincided with the 4-inch operational range of the jack. The output signal was about ±5 volts for the displacement of −1 to +3 inches. When subjected to a temperature gradient, the LVDT output voltage drifts; however, it returns to the original level when the LVDT

temperature becomes uniform again. To avoid this problem, the LVDT's are mounted on the stepper motor mounting frame using thermally insulated blocks. The output signal from each LVDT is sent to both the data acquisition unit of the adaptive wall control computer and the wall protection system. These components are described in subsequent sections of this report.

Wall static pressures are measured along a row of static-pressure orifices on the flexible wall centerline. Pressure orifices are located at each jack station and at the entrance to the test section (station −31.25). The orifices on each flexible wall are connected to a dedicated scanivalve. A conventional strain-gauge transducer is not used in the scanivalve because of the large range of static pressure associated with the test section operating pressure (1.2 to 6.0 atmospheres). Instead, capacitance-type, differential pressure transducers are used. Each transducer has a dedicated autoranging signal conditioner with seven ranges. The autoranging capability keeps the analog output signal at a high level even when the transducer is operating at the low end of its range. Full-scale output of the transducer is 100 millivolts. The transducers have a maximum range of ±100 psid with an accuracy of ±0.25 percent of reading from 25 percent of negative full scale to 100 percent of positive full scale.

Two total-pressure probes are mounted in the beginning of the contraction cone in the instrument mounting blocks shown in figure 15. The probes, made from 0.125-inch-diameter tubing, extend 6.00 inches in from the sidewall and 2.00 inches upstream. The two probes are manifolded together to provide the total pressure for the Mach number calculations. The effective measurement station for the total pressure is at station −107.53. An additional total-pressure probe is mounted from the top of the second contraction piece near its exit. The probe extends 1.62 inches down from the top wall and 1.12 inches upstream. This gives the total pressure at station −36.75 to provide a reference pressure for all total-pressure measurements made with differential pressure transducers.

Static-pressure orifices are located on both sidewalls at station −26.75. The orifices are located at ±4.00 and ±2.00 inches from the centerline on the left wall and ±6.00, ±4.00, ± 2.00, and 0 inches from the centerline on the right wall. These orifices were used to measure the static pressure for the Mach number calculations during the shakedown tests and to provide a reference for the static-pressure instrumentation. The orifices located at ±6.00 inches were influenced by the flexible wall movement and the flow in the test section corner and are not used. Different combinations of static-pressure orifices in the test section were evaluated for use as the static pressure for the Mach number calculations and for use as a reference pressure for all static-pressure measurements made with differential pressure transducers. The static pressure from the orifice on the top wall at station −31.25 was not influenced by the wall movement so it was selected as the static pressure for the Mach number calculations. The four static-pressure orifices at station −26.75 closest to the centerline on the right sidewall have been manifolded together to provide the reference pressure for all differential static-pressure transducers.

Stagnation temperature is measured with a platinum resistance thermometer located at station −105.53. The analog signal from this transducer is converted to digital form by a dedicated digital voltmeter.

Static pressure and total pressure used to compute the free-stream test conditions and the reference pressures used for the differential static- and total-pressure transducers are measured by four dedicated quartz pressure transducers. These differential transducers are referenced to a vacuum to function as absolute pressure devices. Each transducer has a range of ±100 psid and an accuracy of ±0.006 psi ±0.012 percent of the pressure reading. The analog output from each of these transducers is converted to digital form by a dedicated digital voltmeter.

Wall Protection System

A wall protection system was developed to prevent the jacks from driving the flexible walls to shapes that would overstress the wall or exceed the desired jack travel limits. All wall movement commands go through the wall protection system. The wall movement commands can be manually generated by the operator using the 42 toggle switches, one for each jack, or be automatically generated by the adaptive wall control computer. The wall protection system controls a relay which allows the movement commands to be transmitted to the motor power supplies. A photograph of this system is presented in figure 20 and a block diagram is presented in figure 21. The system is built around a microprocessor with an analog input interface and a digital output interface. The microprocessor acquires the output signal from each LVDT through the analog input interface and converts the signal to wall displacement in inches. The wall displacements are used to determine the second derivative of the wall shape. For small slopes, the second derivative is directly related to the wall radius of curvature. Limits have been placed on the radius of curvature of the wall as a function of the wall thickness. The microprocessor computes the local radius of curvature at each jack and at the wall

attachment point. If the radius of curvature of the wall exceeds the limit or the wall displacement reaches the design limit, the microprocessor commands a control relay to open. The open relay prevents movement commands from reaching the motor power supplies. The microprocessor displays the number of the jack which has reached a limit as well as the limit type in the LED display panel mounted above the microprocessor. It also sends the same information to the adaptive wall control computer. An override feature is available for recovery from such limit conditions.

Adaptive Wall Control Computer

A minicomputer is used to control the activities associated with the adaptive wall test section. It has a 16-bit word size and 512 kilobytes of random access memory. The computer has a dedicated fixed disk drive, a removable disk drive, an alphanumeric CRT, a medium-resolution color CRT, a data acquisition unit, and a general purpose input-output system. The fixed disk storage is 133 megabytes and the removable disk storage is 67 megabytes. The alphanumeric CRT serves as the operator's console and provides all interactive communication between the operator and the various software tasks. The color CRT provides the operator a graphic and tabular representation of the wall shape, pressure distribution, and Mach number distribution. The data acquisition unit digitizes the analog inputs from the LVDT's and the wall pressure transducers and provides an interface for the digital signal from the digital voltmeter dedicated to the reference static pressure. Additional details of the data acquisition unit are provided below. The general input-output system provides the digital interfaces to the scanivalve controller and the wall protection system. It also provides a pulse output to the stepping motor controllers to move the jacks under computer control. A link connects the adaptive wall control computer to the research data acquisition computer for the 0.3-m TCT. The two computers share two nine-track tape drives and a line printer.

A 64-channel, analog data acquisition unit measures the LVDT outputs and the pressure transducer signal conditioner gain and signal outputs. The range of each input channel is selected by the adaptive wall control computer. Six input ranges are available: ± 4, ± 8, ± 16, ± 32, ± 65, and ± 131 millivolts. Since the LVDT output signal range exceeds the largest range available on the data acquisition unit, a 0.021845:1 signal attenuator circuit was added to each channel. The data acquisition unit can scan and digitize the inputs at 50 000 samples per second. Each channel has a 10-hertz, low-pass filter to reduce the effects of noise. Because of command signals to and from the unit and the speed of the interface to the adaptive wall control computer, the effective rate is 32 000 samples per second. Fourteen bits from the analog-to-digital converter are used to give a measurement accuracy of 1 part in 8191.

A 16-channel digital data acquisition unit measures the output from the digital voltmeter for the static reference pressure transducer. This digital reading is recorded along with the digitized analog readings from the signal conditioner gain and signal for each port of the scanivalve and from each LVDT. The differential pressure for each port can then be properly converted to an absolute pressure.

Adaptive Wall Test Section Operating Strategy

The adaptive wall test section concept attempts to eliminate the interference from the test section walls at its source. It does this by modifying the flow field at the test section boundaries such that the flow field in the vicinity of the model approaches that which would be obtained for "free air" conditions. A sketch of the assumed flow field used for development of the adaptive wall concept is shown in figure 22. The flow field is split into two regions: the "real" flow field inside a control surface and the "imaginary" flow field extending from the control surface to infinity. The wind tunnel generates the real flow field where there are compressibility, viscous, and rotational effects present. Computational fluid dynamics simulates the imaginary flow field. Potential flow methods can be used if the imaginary flow field is assumed to be irrotational. The adaptive wall concept requires that the real flow field match the imaginary flow field at the control surface. This requirement is satisfied if two independent flow parameters are matched locally on the control surface.

The wall adaptation strategy used to match the parameters for the shakedown tests is described in reference 7. For the 0.3-m TCT, the two independent parameters to be matched at the control surface are the flow speed and the flow direction. The flow speed is determined from the local wall static-pressure coefficient. The flow direction is determined from the local slope of the effective wall shape (wall plus boundary layer). The adaptation technique uses an iterative procedure to determine the required wall shape. The wall static-pressure distribution and shape are measured. The pressure distribution is converted to a "measured" or real velocity perturbation. The measured or real wall shape is used as the boundary condition for the potential flow solver which computes the imaginary flow field. Thus, the real wall shape and slope are identical to the

computed or imaginary wall shape and slope. The potential flow solver provides a computed or imaginary velocity perturbation. The difference in the measured and computed velocity perturbations is used to compute five parameters: the average pressure coefficient error at the top wall, the average pressure coefficient error at the bottom wall, the average pressure coefficient error on the model, the angle of attack induced at the model, and the camber induced at the model. Each of these parameters is compared with a maximum allowable value for convergence. If each parameter is less than the maximum allowable value, the wall position is assumed to induce an acceptably small level of interference and the iterative process terminates. The research measurements for the airfoil model are then recorded along with the top and bottom wall pressures and positions. If any parameter exceeds the maximum allowable value, then a new wall shape is computed as follows. The wall is treated as a vortex sheet, the strength of which is determined by the difference between the measured and computed tangential velocity perturbations. The downwash induced by the sheet is evaluated at each jack station and the change in wall slope needed to redirect the free-stream velocity to cancel the induced downwash is calculated. This change in wall slope is integrated to determine the change in wall shape. The flexible walls are positioned to the new wall shape and the iterative process continues.

Preliminary Results

Shakedown tests were first conducted with the test section empty. The Mach number was varied from 0.2 to 0.9 at Reynolds numbers per foot from 10×10^6 to 100×10^6. A sample of the test section Mach number distribution for a nominal Mach number of 0.7 is presented in figure 23. Initial tests with the top and bottom flexible walls straight (at the undeflected shape) showed a Mach number gradient through the test section as expected (fig. 23(a)). The Mach number generally increases in the streamwise direction although there is considerable scatter in some of the measurements. A single scanivalve and a pressure transducer were used for the top wall and for the bottom wall. Since the scatter does not occur at the same port (streamwise position) and there were no detectable leaks, the scatter is not attributable to the scanivalve or the transducer. It is probably attributable to the waviness of the wall and free play in the wall positioning system. The increase in the boundary-layer-displacement thickness leads to an increase in the local Mach number until the diverging transition portion at the end of the test section is reached. There, the Mach number decreases as the cross-sectional area rapidly increases. Diverging the walls linearly reduced the Mach number gradient significantly as shown in figure 23(b). Further refinements in the flexible wall displacement were tried. The refined shape, presented in figure 23(c), was rather wavy and reduced the scatter in the results. However, when the refined shape was used as the reference condition for tests with a model, the commanded wall movements frequently led to wall shapes which could not be obtained with the current wall positioning hardware. The linearly diverging wall shapes were selected as the reference conditions for tests with a model.

The noise level in the adaptive wall test section should be less than the noise in the previous slotted wall test section because the adaptive wall test section has no slots, has a greater contraction ratio, the distance from the fan to the test section and from the LN_2 injection to the test section was increased, and the divergence angle in the high-speed diffuser was reduced. Fluctuating sidewall pressure measurements in the adaptive wall test section were obtained at several Mach numbers. These unpublished fluctuating sidewall pressure results have been excerpted from the work of W. B. Igoe for a proposed doctoral dissertation to be submitted to the George Washington University. The fluctuating sidewall pressures for the slotted wall test section were reported in reference 8. These results are compared in figure 24. The adaptive wall test section fluctuating pressure level is about one half the level measured in the 8- by 24-inch slotted test section. This reduction is attributable to the removal of the slots, the increase in contraction ratio, and the improved high-speed diffuser.

Several airfoil models with chords ranging from 6.0 inches to 13.0 inches were tested during the shakedown tests. The test Mach number ranged from 0.3 to 0.8 and the chord Reynolds number ranged from 3×10^6 to 72×10^6. The shakedown tests were designed to check out the test section hardware, software, and operational procedures with typical airfoil models. Experiences with some of these typical models are presented in reference 9. One of the models had a 9.0-inch chord and a CAST 10-2/DOA 2 airfoil section. The resulting ratio of test section height to model chord of 1.4 will lead to substantial wall interference if the walls are not properly adapted. For this test, the walls were considered to be properly adapted if the average error in C_p on each wall was less than 0.01, the induced error in α was less than 0.015°, the induced camber error was less than 0.07, and the average error in C_p along the model chord was less than 0.007. The adaptive wall results without any corrections for residual interference were reported in reference 10. A sample airfoil chordwise pressure distribution with the

associated adapted wall shape and wall pressure distribution is presented in figure 25. A sample of the integrated force and moment coefficients is presented in figure 26. These adaptive wall results are compared with test results on the same model in a relatively large, conventional test section where the ratio of height to chord was 6.7. The conventional test section results were corrected for top and bottom wall interferences and were reported in reference 11. These corrected results were expected to have negligible interference from the top and bottom walls and are used as a baseline to assess the interference in the adaptive wall test section. The agreement is remarkable considering the differences between the two test sections used. These results demonstrate that the adaptive wall test section dramatically reduces the wall interference.

Concluding Remarks

An adaptive wall test section has been installed in the circuit of the Langley 0.3-Meter Transonic Cryogenic Tunnel. The various features of the test section as well as modifications to the tunnel circuit have been discussed. Shakedown tests demonstrated successful operations over a Mach number range from 0.3 to 0.8 and a chord Reynolds number range from 3×10^6 to 72×10^6. The results from the shakedown tests demonstrated that the noise level is lower in the adaptive wall test section than in the previous slotted wall test section. The uncorrected, adaptive wall test section results are in good agreement with corrected, conventional test section results. Adaptive wall test sections can dramatically reduce the wall interference for two-dimensional airfoil tests.

NASA Langley Research Center
Hampton, VA 23665-5225
April 28, 1989

References

1. Mokry, M.; Chan, Y. Y.; and Jones, D. J.: *Two-Dimensional Wind Tunnel Wall Interference.* AGARD-AG-281, Nov. 1983.
2. Sears, W. R.: Self-Correcting Wind Tunnels. *Aeronaut. J.*, vol. 78, no. 758/759, Feb./Mar. 1974, pp. 80–89.
3. Tuttle, Marie H.; and Mineck, Raymond E.: *Adaptive Wall Wind Tunnels—A Selected, Annotated Bibliography.* NASA TM-87639, 1986.
4. Wolf, S. W. D.: *Self Streamlining Wind Tunnel—Further Low Speed Testing and Final Design Studies for the Transonic Facility.* NASA CR-158900, 1978.
5. Ladson, Charles L.; and Ray, Edward J.: *Evolution, Calibration, and Operational Characteristics of the Two-Dimensional Test Section of the Langley 0.3-Meter Transonic Cryogenic Tunnel.* NASA TP-2749, 1987.
6. Johnson, Charles B.; Murthy, A. V.; and Ray, Edward J.: *A Description of the Active and Passive Sidewall-Boundary-Layer Removal Systems of the 0.3-Meter Transonic Cryogenic Tunnel.* NASA TM-87764, 1986.
7. Wolf, Stephen W. D.; and Goodyer, Michael J.: *Predictive Wall Adjustment Strategy for Two-Dimensional Flexible Walled Adaptive Wind Tunnel—A Detailed Description of the First One-Step Method.* NASA CR-181635, 1988.
8. Johnson, C. B.; Johnson, W. G., Jr.; and Stainback, P. C.: A Summary of Reynolds Number Effects on Some Recent Tests in the Langley 0.3-Meter Transonic Cryogenic Tunnel. SAE Tech. Paper Ser. 861765, Oct. 1986.
9. Wolf, Stephen W. D.; and Ray, Edward J.: *Highlights of Experience With a Flexible Walled Test Section in the NASA Langley 0.3-Meter Transonic Cryogenic Tunnel.* NASA TM-101491, 1988.
10. Mineck, Raymond E.: *Wall Interference Tests of a CAST 10-2/DOA 2 Airfoil in an Adaptive-Wall Test Section.* NASA TM-4015, 1987.
11. Chan, Y. Y.: *Wind Tunnel Investigation of CAST-10-2/DOA-2 12% Supercritical Airfoil Model.* LTR-HA-5×5/0162, National Aeronautical Establ., National Research Council of Canada, May 1986.

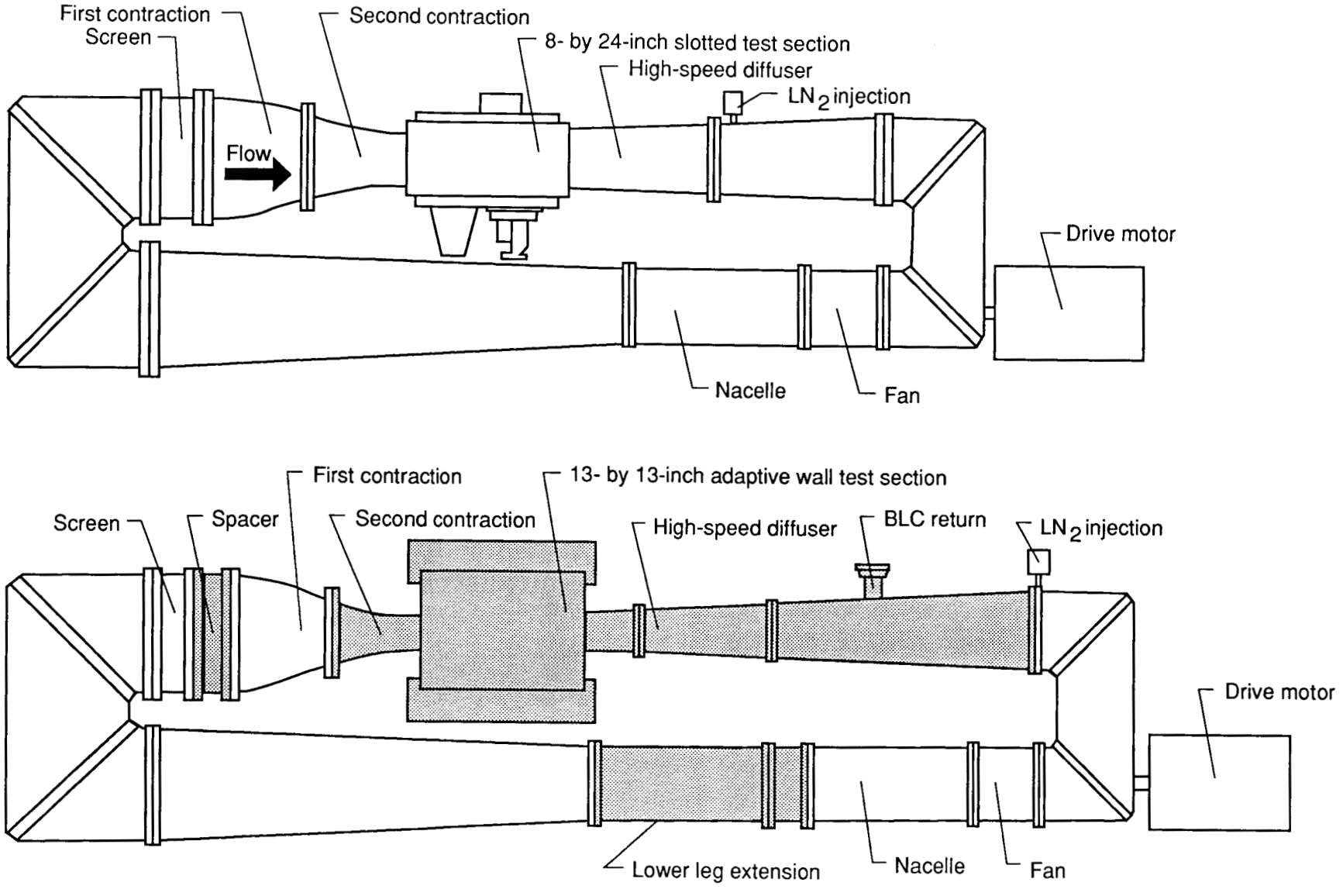

Figure 1. Changes to Langley 0.3-Meter Transonic Cryogenic Tunnel circuit.

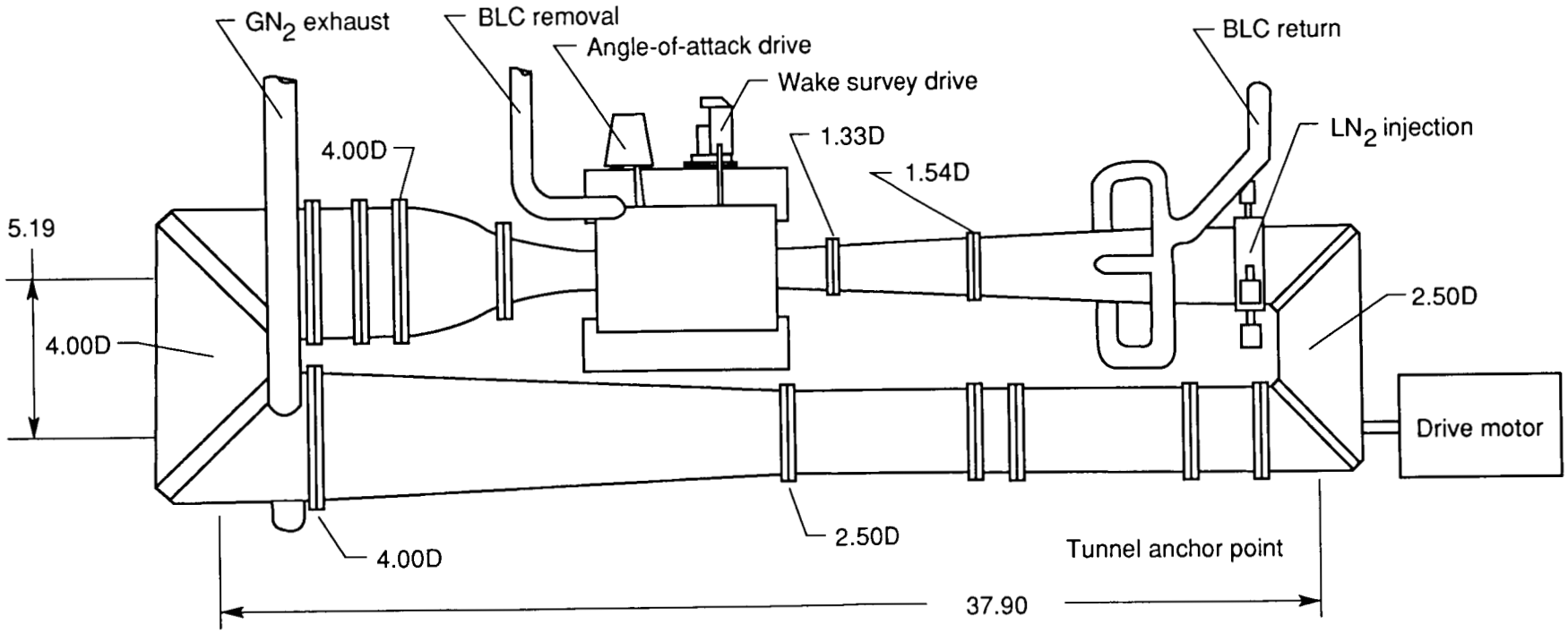

Figure 2. Sketch of 0.3-m TCT circuit with 13- by 13-inch adaptive wall test section. Dimensions are in feet.

ORIGINAL PAGE
BLACK AND WHITE PHOTOGRAPH

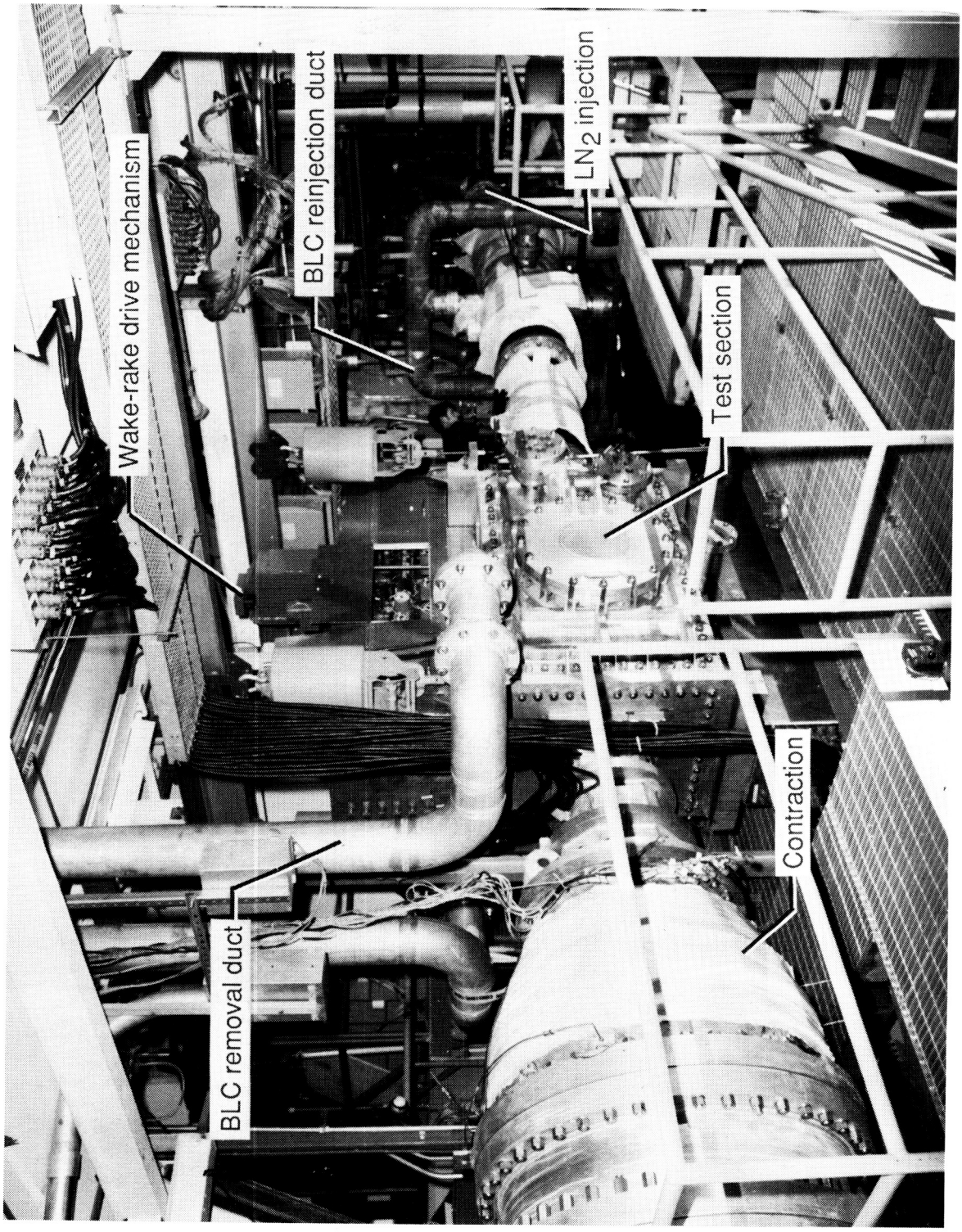

L-89-45

Figure 3. Photograph of upper leg of 0.3-m TCT with 13- by 13-inch adaptive wall test section.

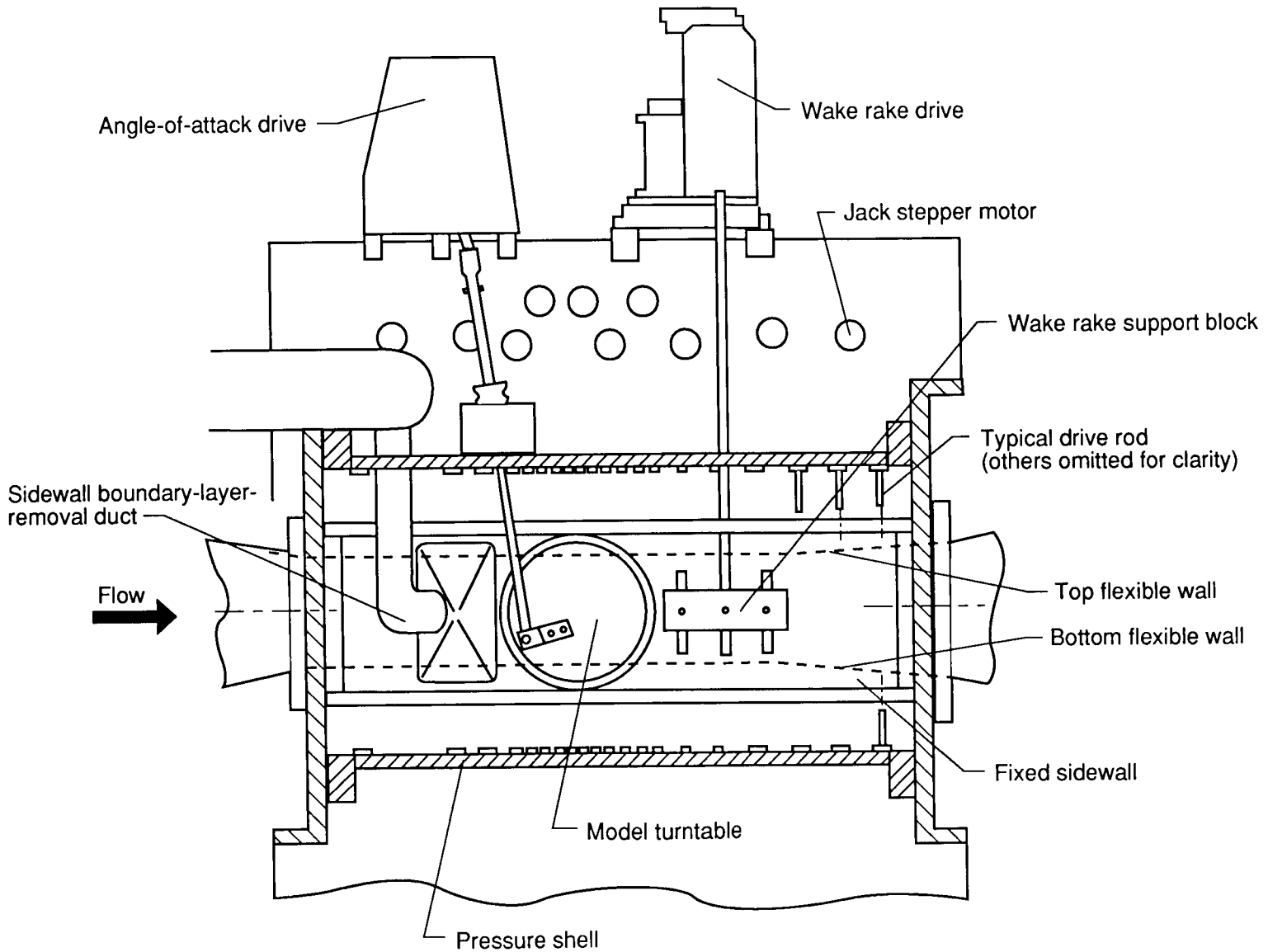

Figure 4. Layout of 13- by 13-inch adaptive wall test section with plenum sidewall removed.

ORIGINAL PAGE
BLACK AND WHITE PHOTOGRAPH

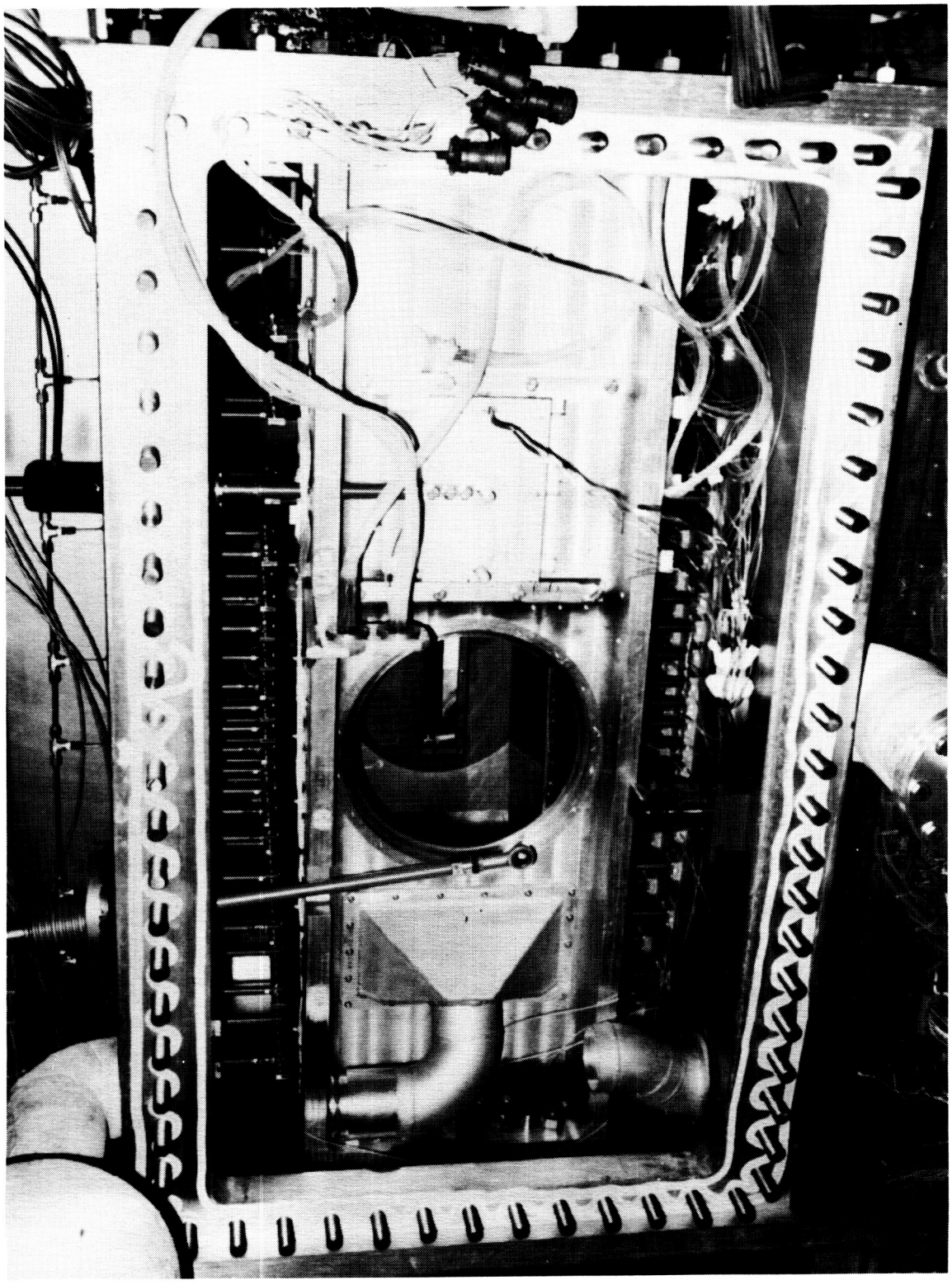

L-87-8385

Figure 5. Photograph of flow region of adaptive wall test section with plenum sidewall removed.

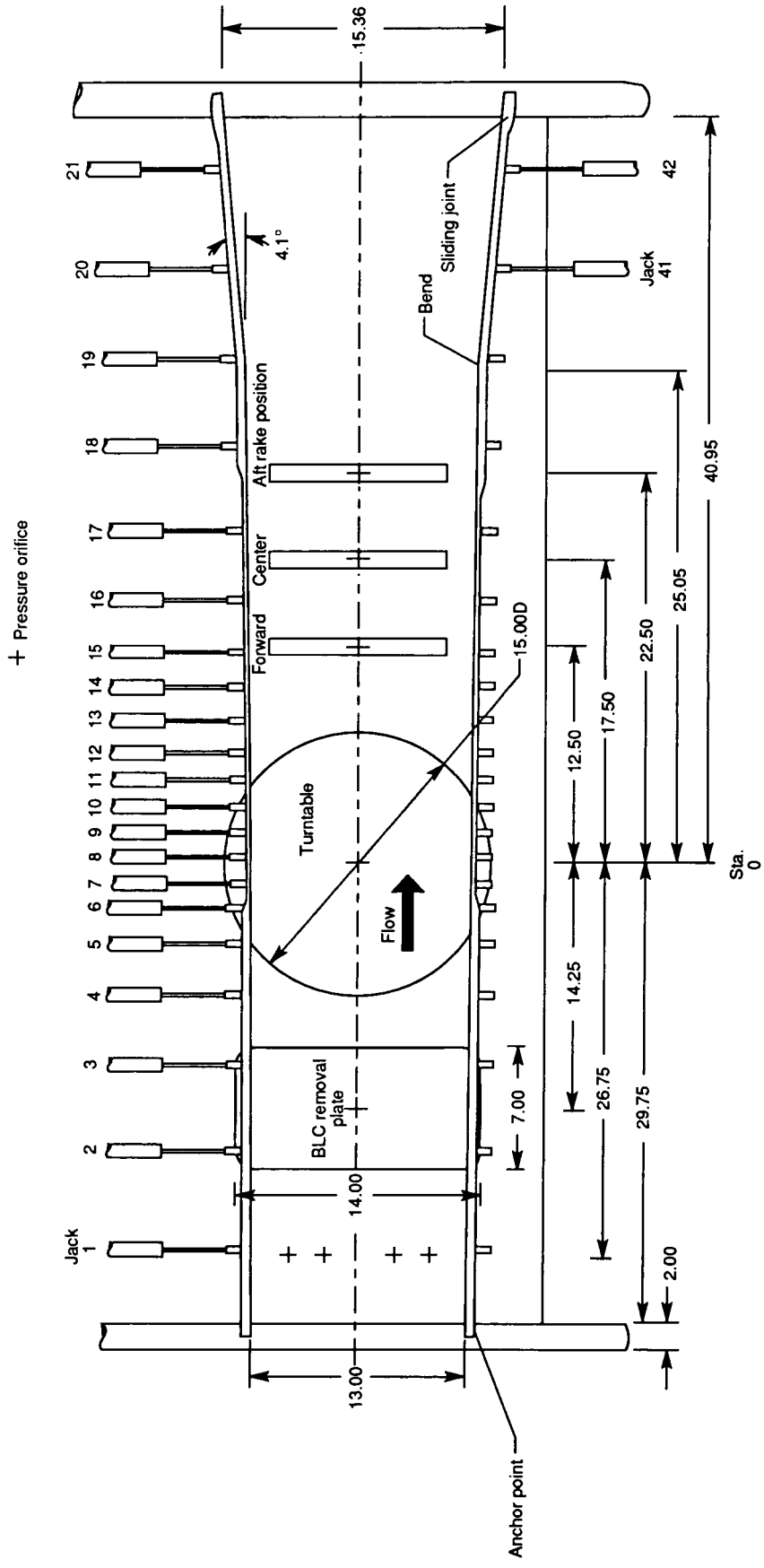

Figure 6. Details of flow region of 13- by 13-inch adaptive wall test section. All dimensions are in inches; some lower wall jacks omitted for clarity.

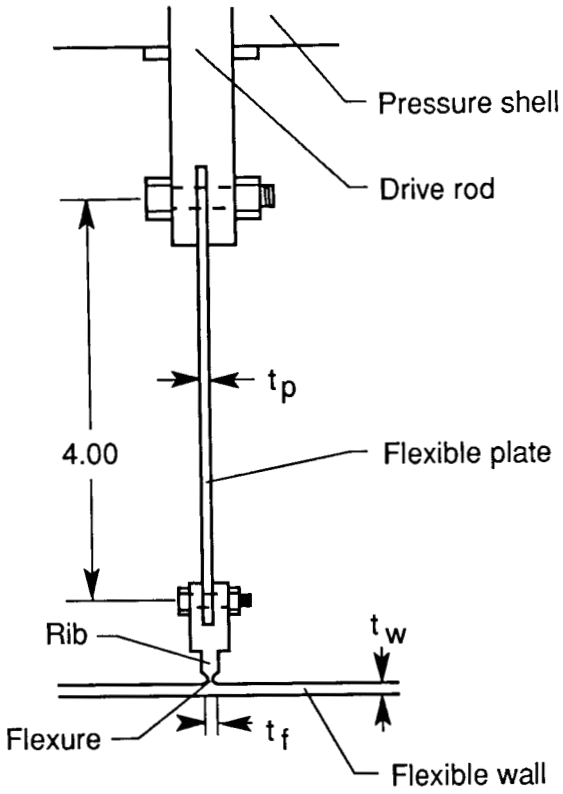

Jack	x sta., in.	t_w, in.	t_f, in.	t_p, in.
1, 22	-26.00	0.125	0.125	0.125
2, 23	-20.25	.125	.125	.125
3, 24	-15.25	.125	.125	.125
4, 25	-11.25	.125	.125	.125
5, 26	-8.25	.125	.125	.125
6, 27	-6.25	.062	.062	.094
7, 28	-4.75	.062	.062	.094
8, 29	-3.25	.062	.062	.094
9, 30	-1.75	.062	.062	.094
10, 31	-.25	.062	.062	.094
11, 32	1.25	.062	.062	.094
12, 33	2.75	.062	.062	.094
13, 34	4.75	.062	.062	.094
14, 35	6.75	.062	.062	.094
15, 36	8.75	.062	.062	.094
16, 37	11.75	.062	.062	.094
17, 38	15.75	.062	.062	.094
18, 39	20.75	.125	.125	.125
19, 40	25.75	.125	.125	.125
20, 41	30.75	.125	.125	.125
21, 42	36.25	.125	.125	.125

Figure 7. Details of wall attachment system. All dimensions are in inches.

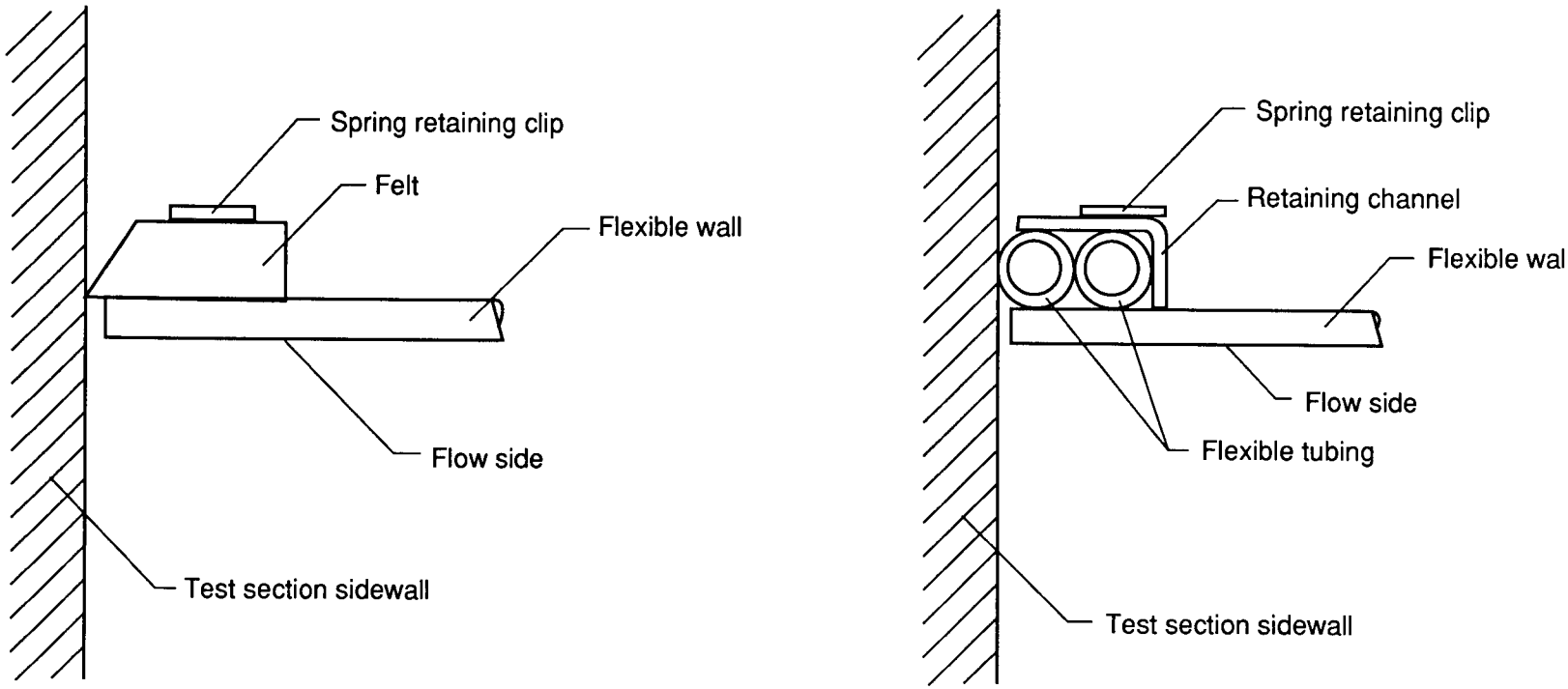

(a) Original felt seal.

(b) Current tubing seal.

Figure 8. Corner seals between sidewalls and flexible walls.

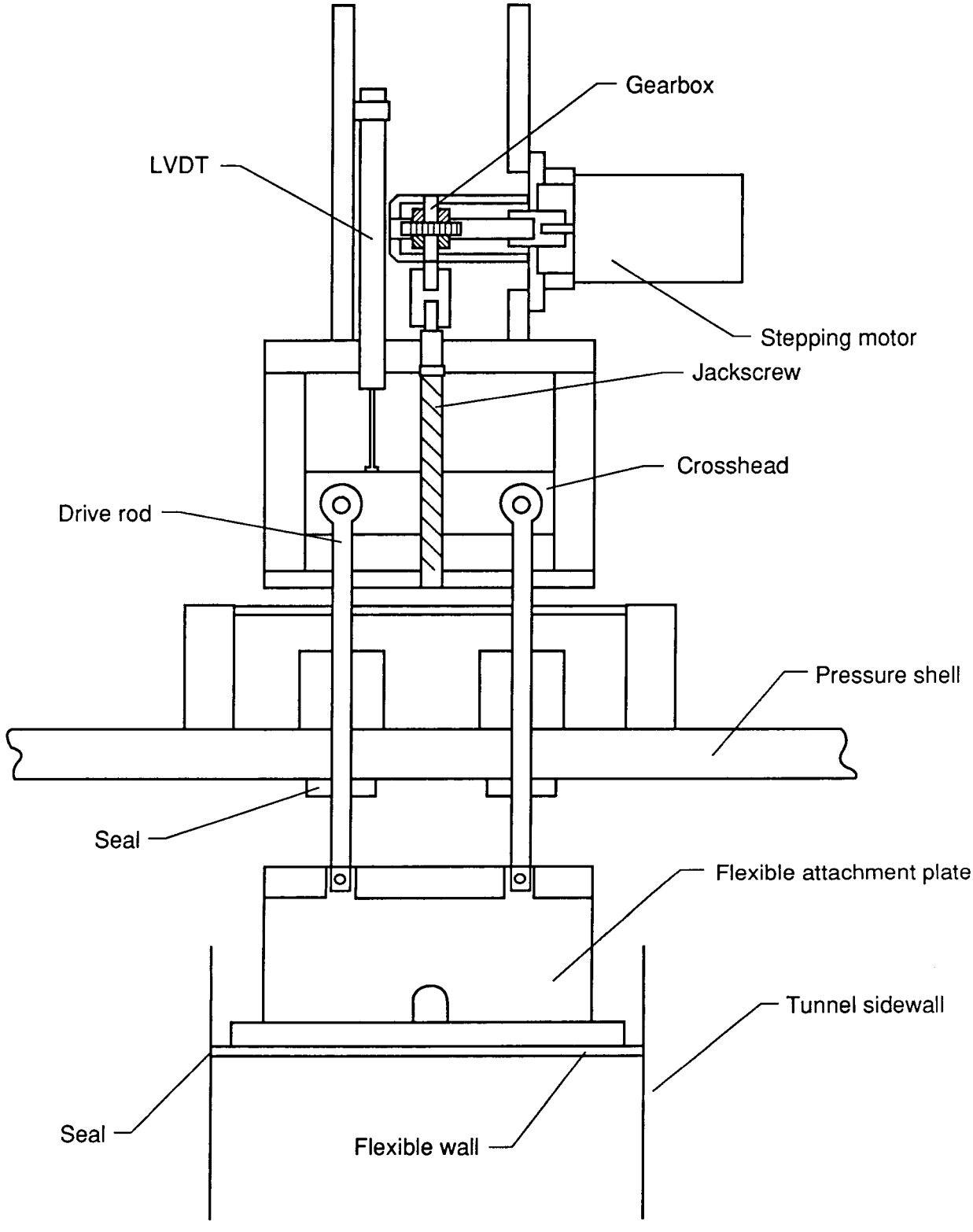

Figure 9. Sketch of wall positioning system.

ORIGINAL PAGE
BLACK AND WHITE PHOTOGRAPH

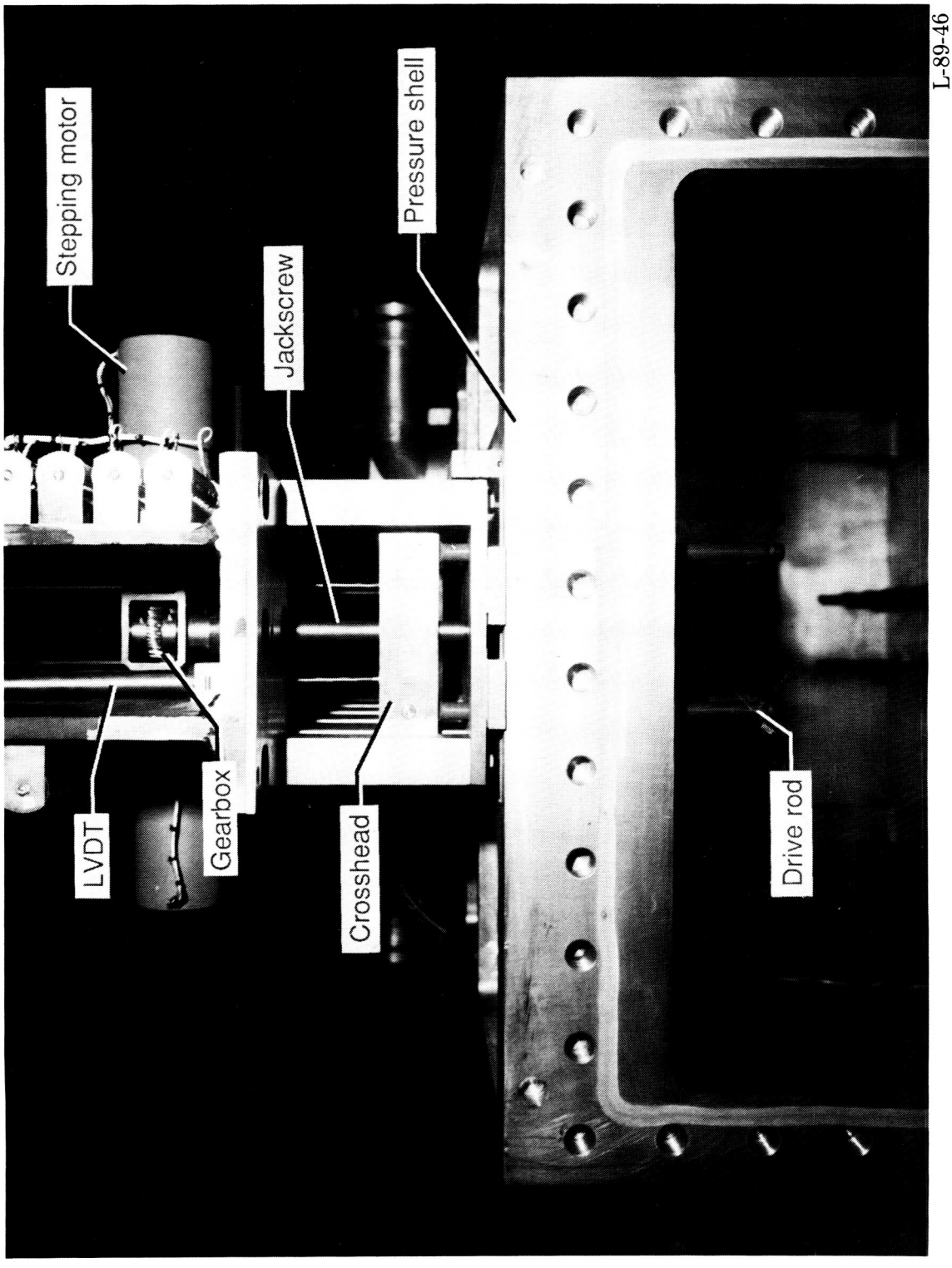

Figure 10. Photograph of wall positioning system.

ORIGINAL PAGE
BLACK AND WHITE PHOTOGRAPH

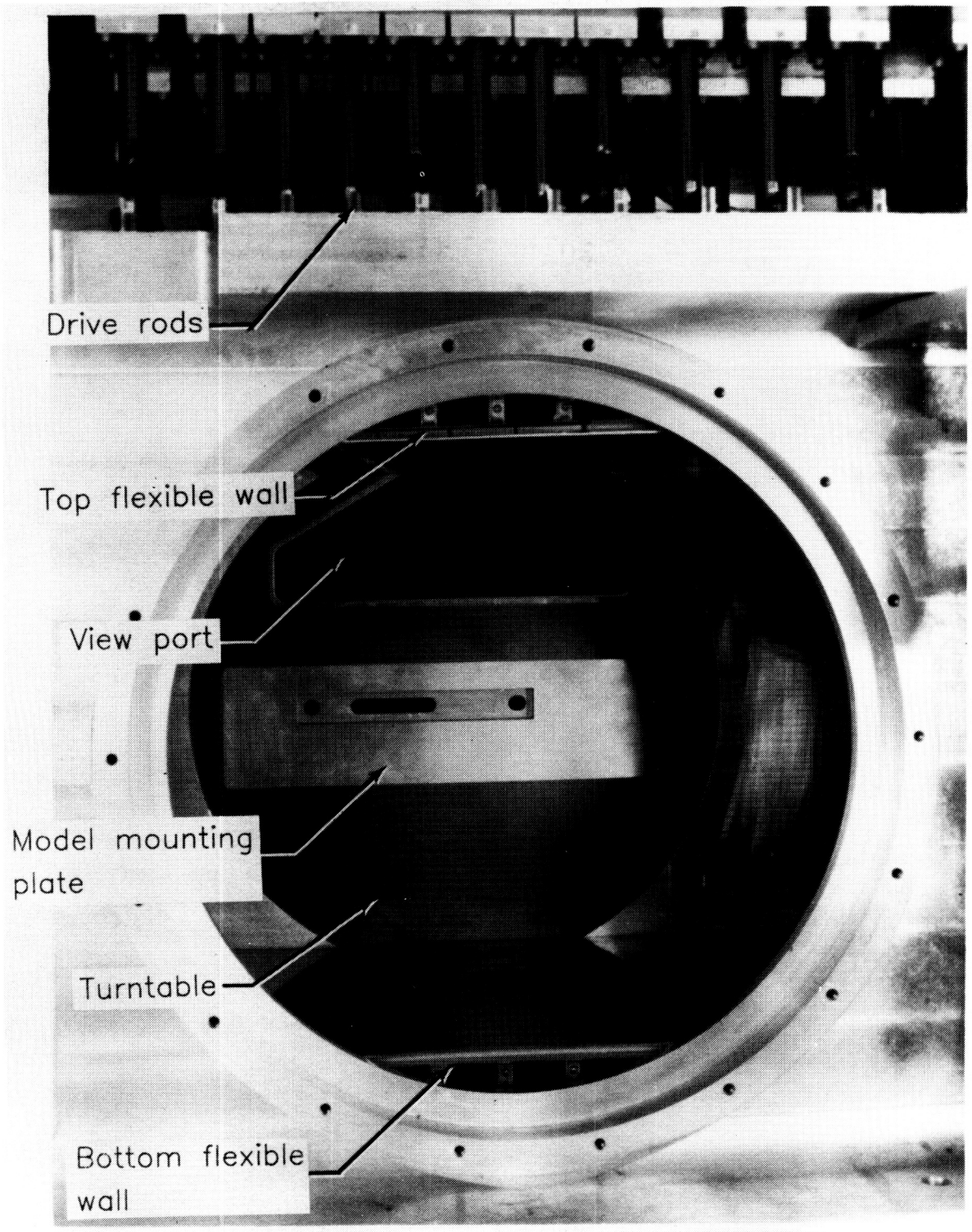

L-87-659

Figure 11. Photograph of region where the model is installed.

ORIGINAL PAGE
BLACK AND WHITE PHOTOGRAPH

L-89-47

(a) Model just prior to installation.

Figure 12. Photographs of model installation.

ORIGINAL PAGE
BLACK AND WHITE PHOTOGRAPH

L-89-48

(b) Model after installation.

Figure 12. Concluded.

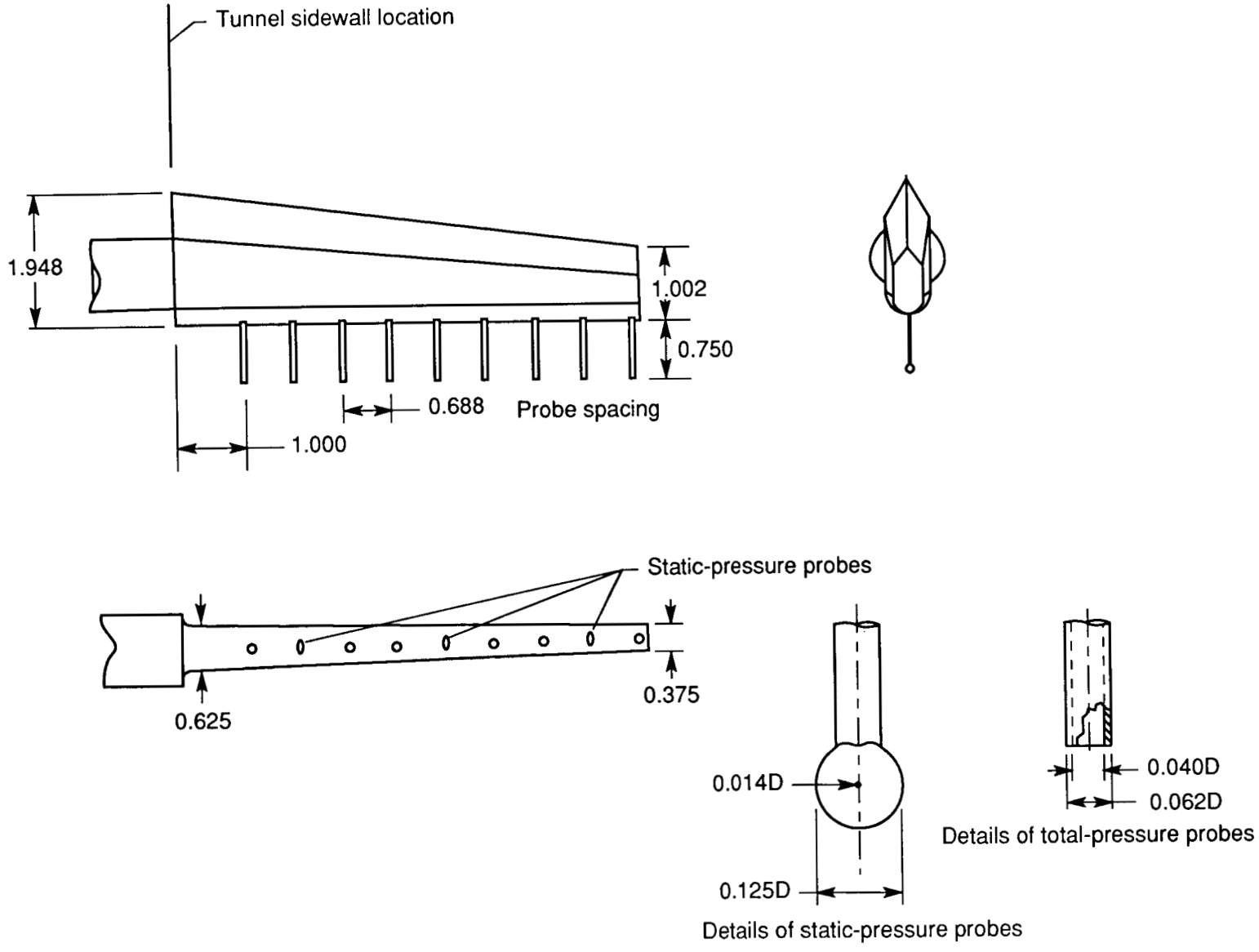

Figure 13. Sketch of wake survey probe. All dimensions are in inches.

ORIGINAL PAGE
BLACK AND WHITE PHOTOGRAPH

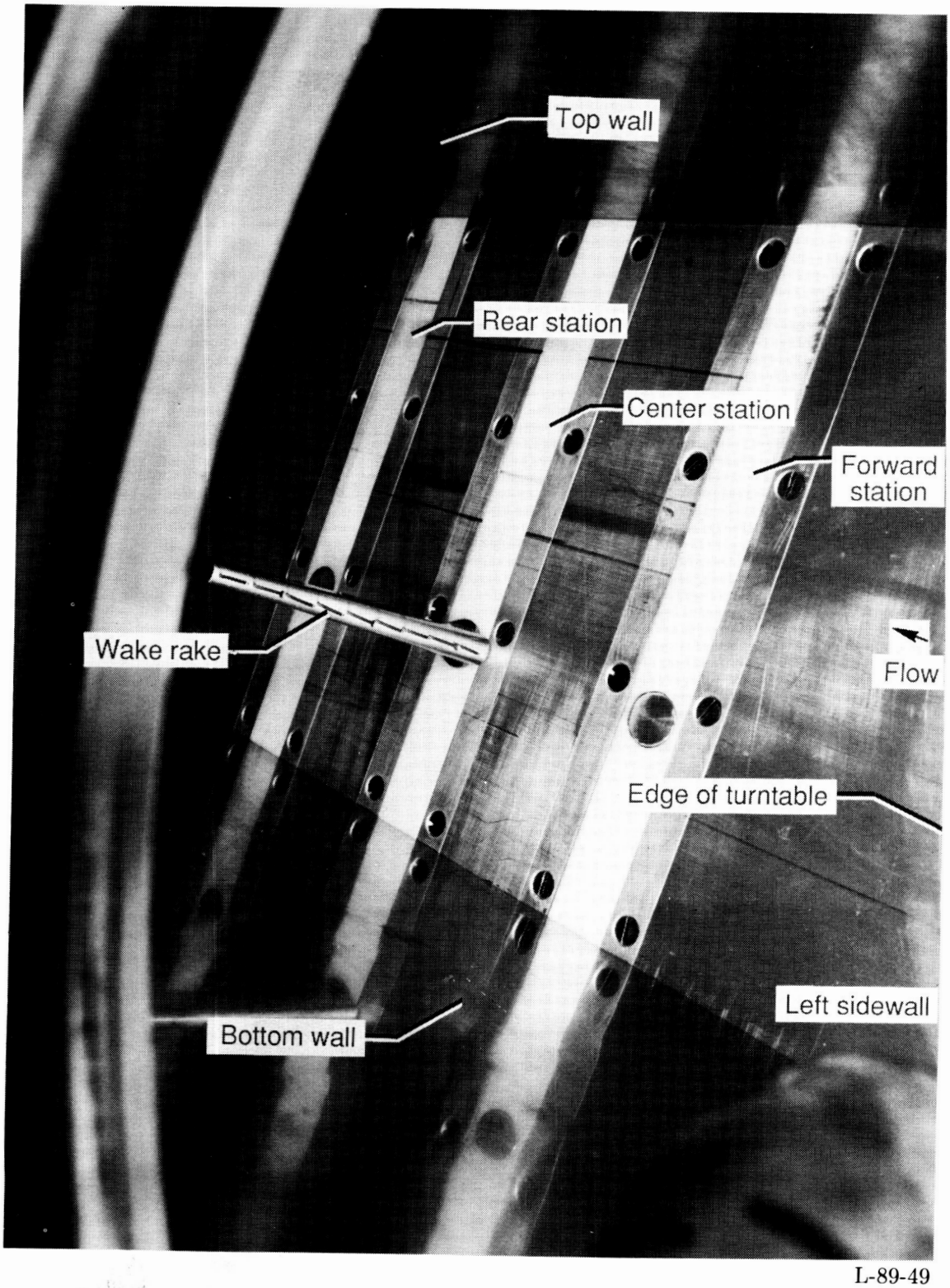

L-89-49

Figure 14. Photograph of wake survey probe mounted in center survey station.

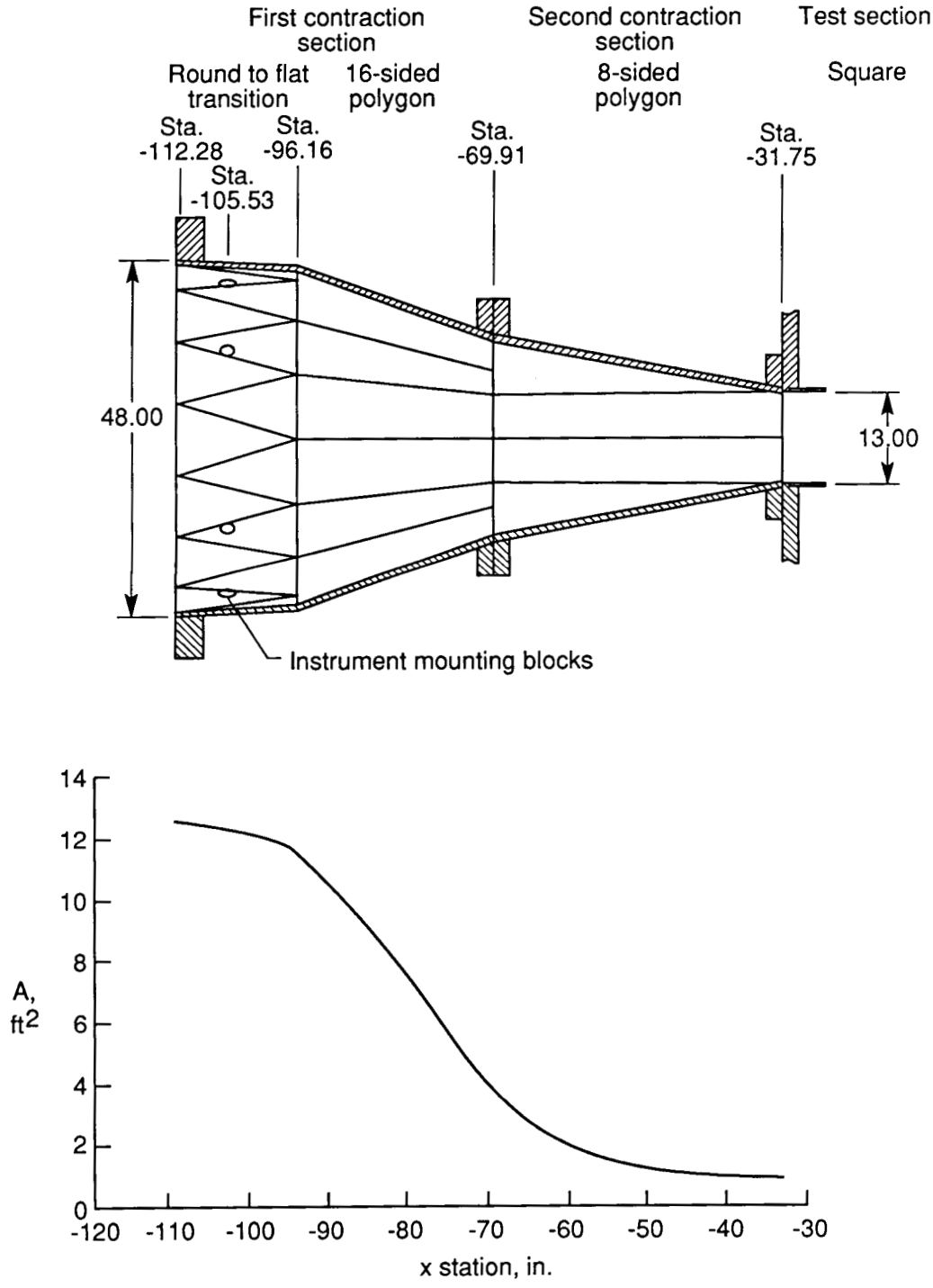

Figure 15. Sketch of contraction section. All dimensions are in inches.

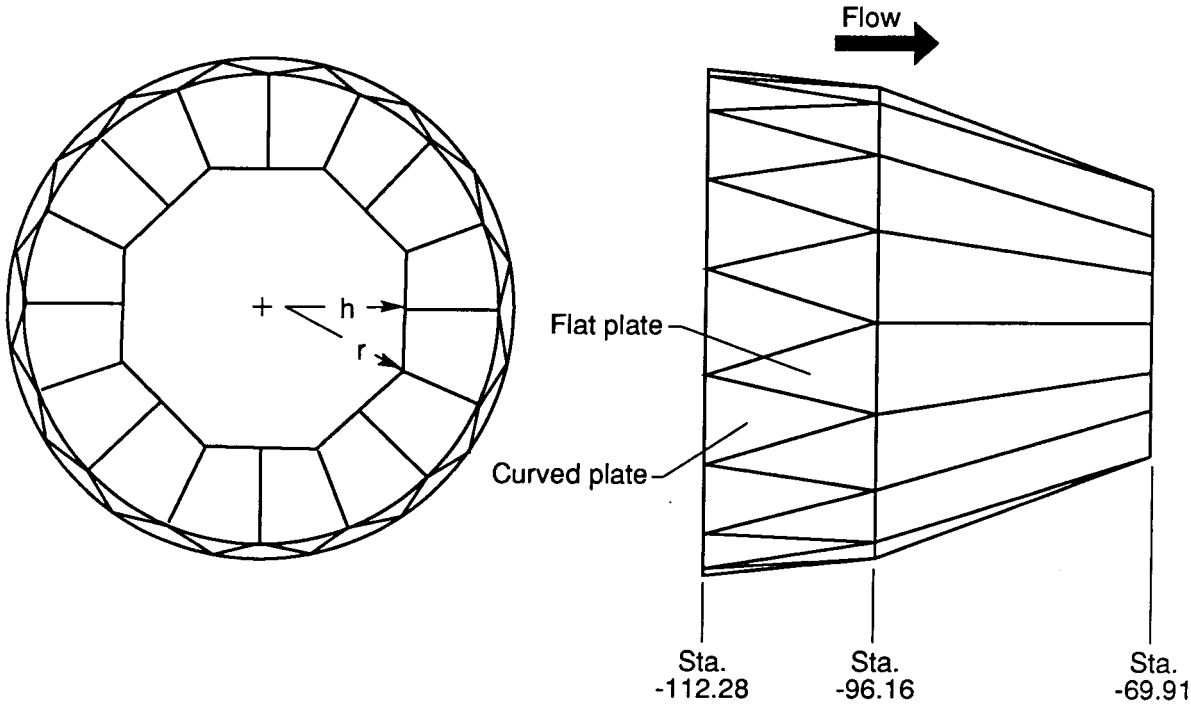

x sta., in.	h, in.	r, in.
-96.36	23.49	23.49
-94.28	23.06	23.06
-92.28	22.53	22.53
-90.28	21.92	21.92
-88.28	21.22	21.28
-86.28	20.48	20.59
-84.28	19.69	19.88
-82.28	18.87	19.17
-80.28	18.01	18.43
-78.28	17.11	17.69
-76.28	16.18	16.94
-74.28	15.28	16.19
-72.28	14.42	15.44
-70.28	13.44	14.46
-69.91	12.68	13.80

Figure 16. Details of the first contraction section.

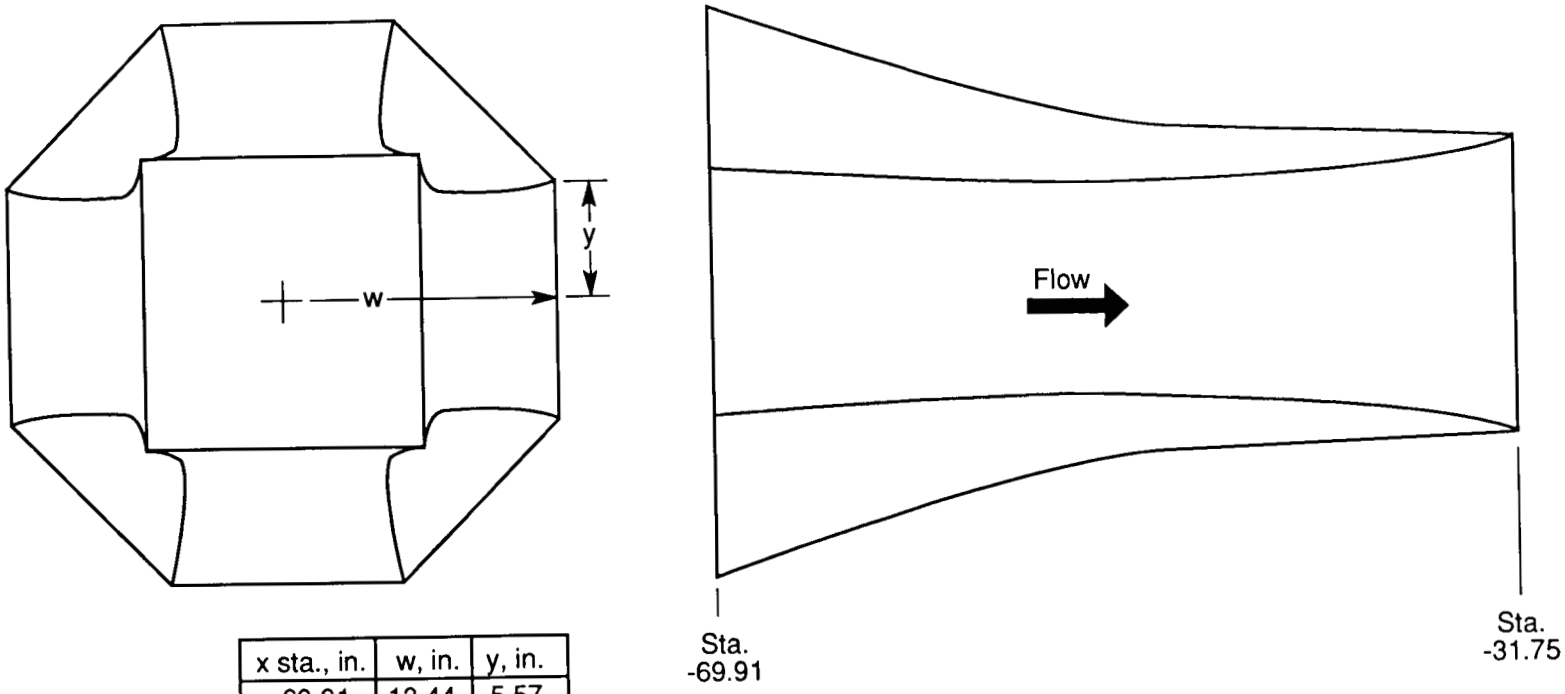

x sta., in.	w, in.	y, in.
-69.91	13.44	5.57
-68.38	12.68	5.44
-67.75	12.43	5.40
-65.11	11.47	5.23
-62.43	10.58	5.07
-59.78	9.76	4.93
-57.08	9.01	4.80
-54.44	8.36	4.71
-51.74	7.83	4.67
-48.98	7.41	4.70
-46.18	7.07	4.78
-43.35	6.83	4.95
-40.52	6.64	5.17
-37.63	6.55	5.51
-34.71	6.50	5.95
-31.75	6.50	6.50

Figure 17. Details of second contraction section.

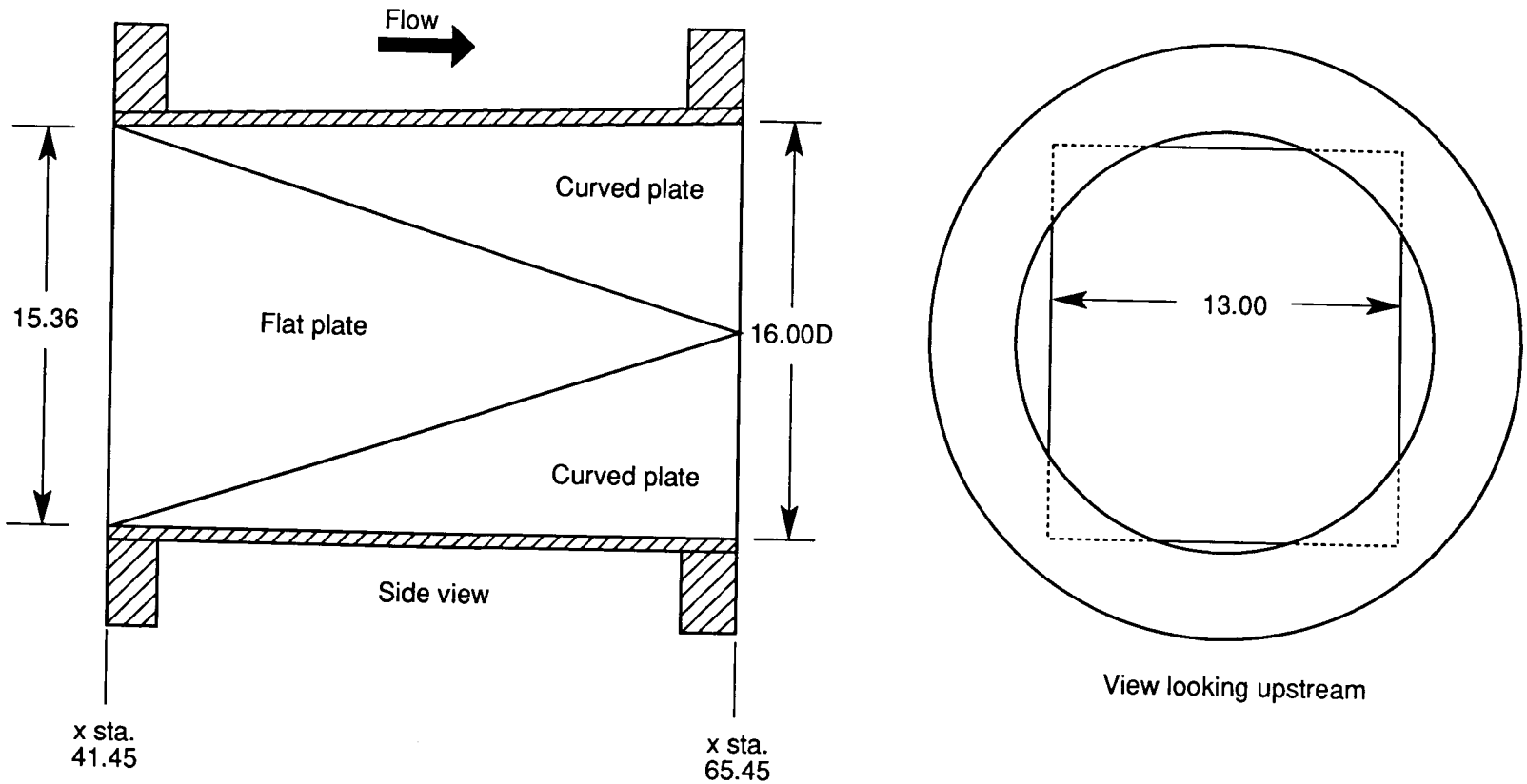

Figure 18. Details of first section of high-speed diffuser. Dimensions are in inches.

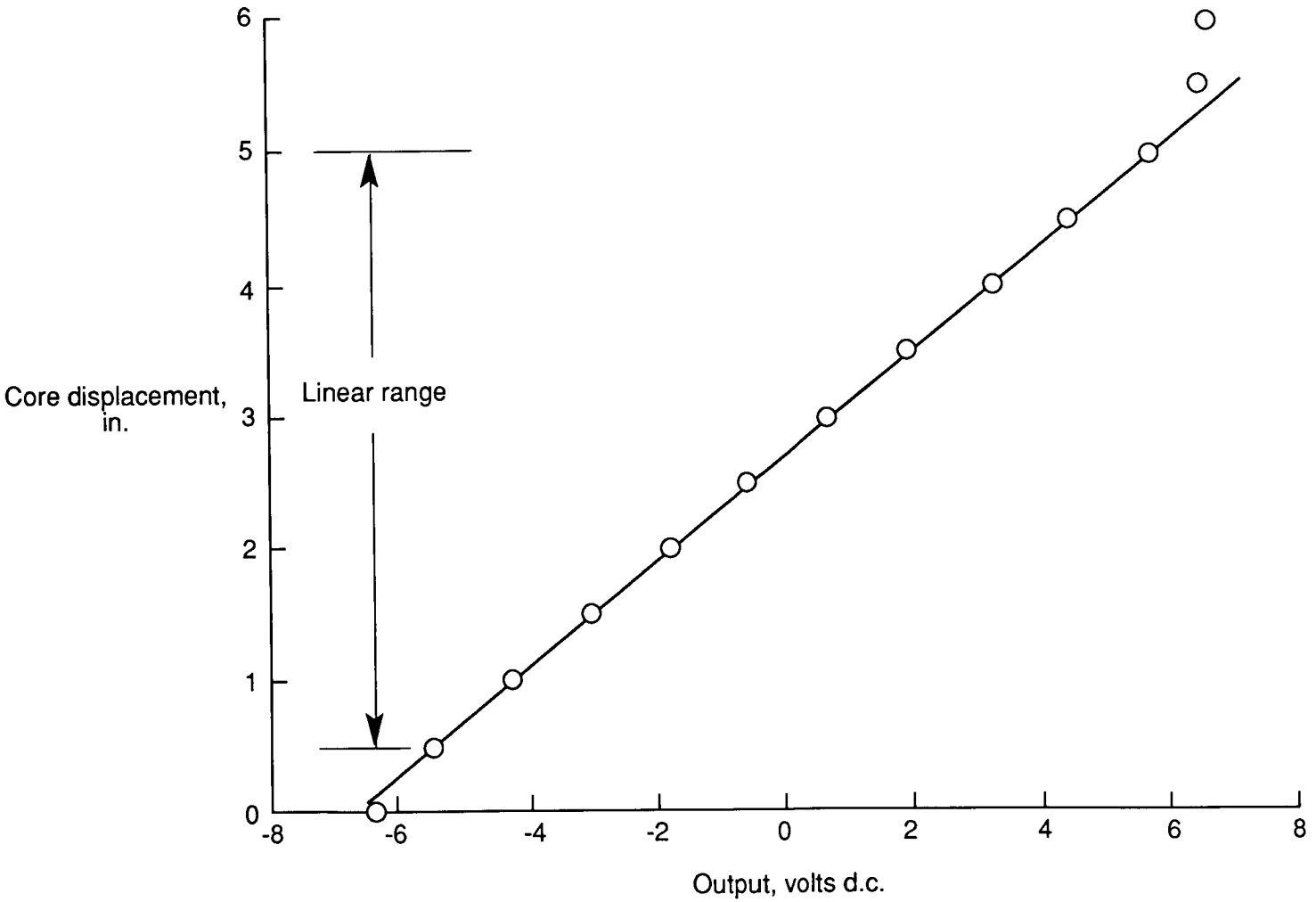

Figure 19. Calibration of typical LVDT.

ORIGINAL PAGE
BLACK AND WHITE PHOTOGRAPH

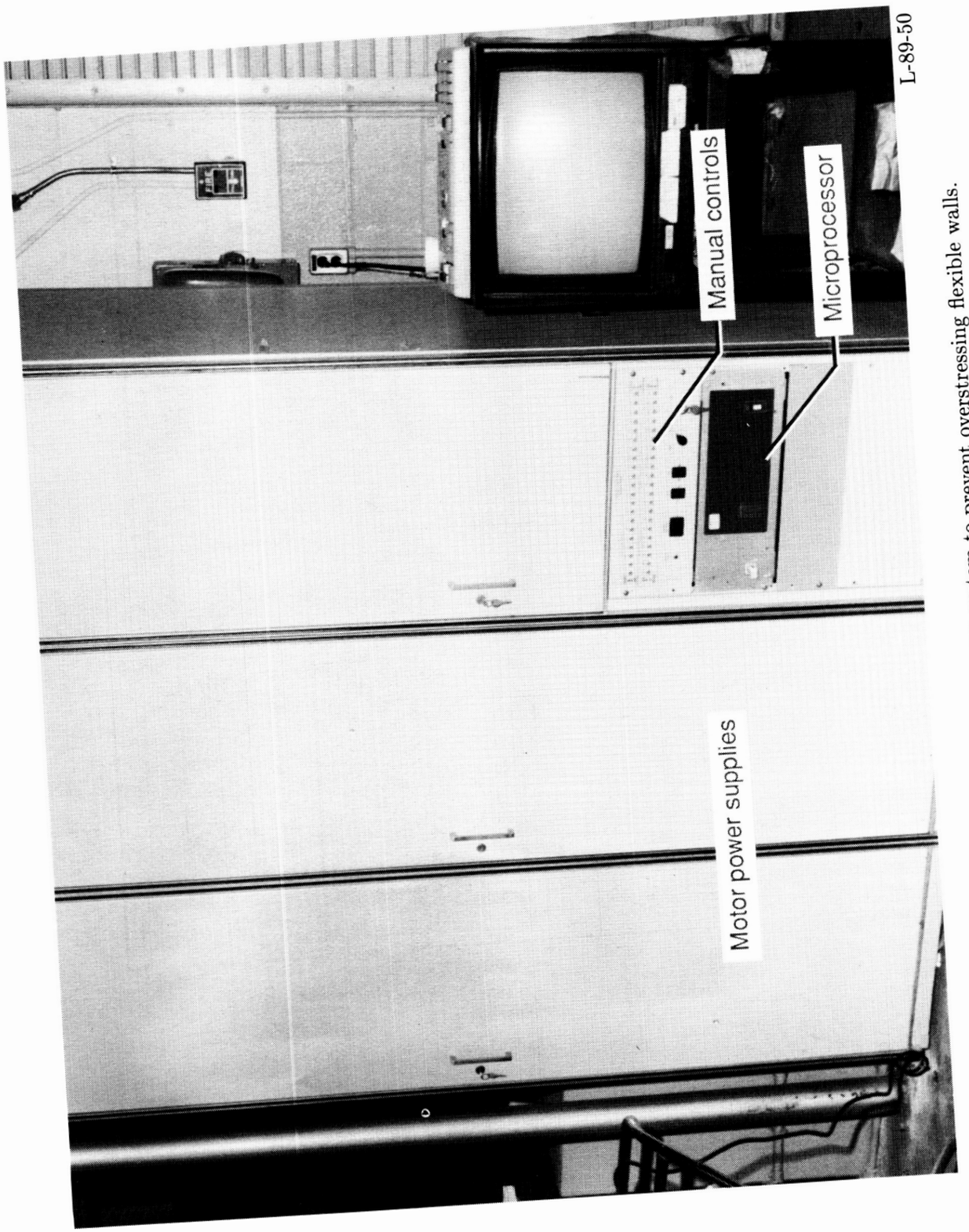

Figure 20. Photograph of microprocessor system to prevent overstressing flexible walls.

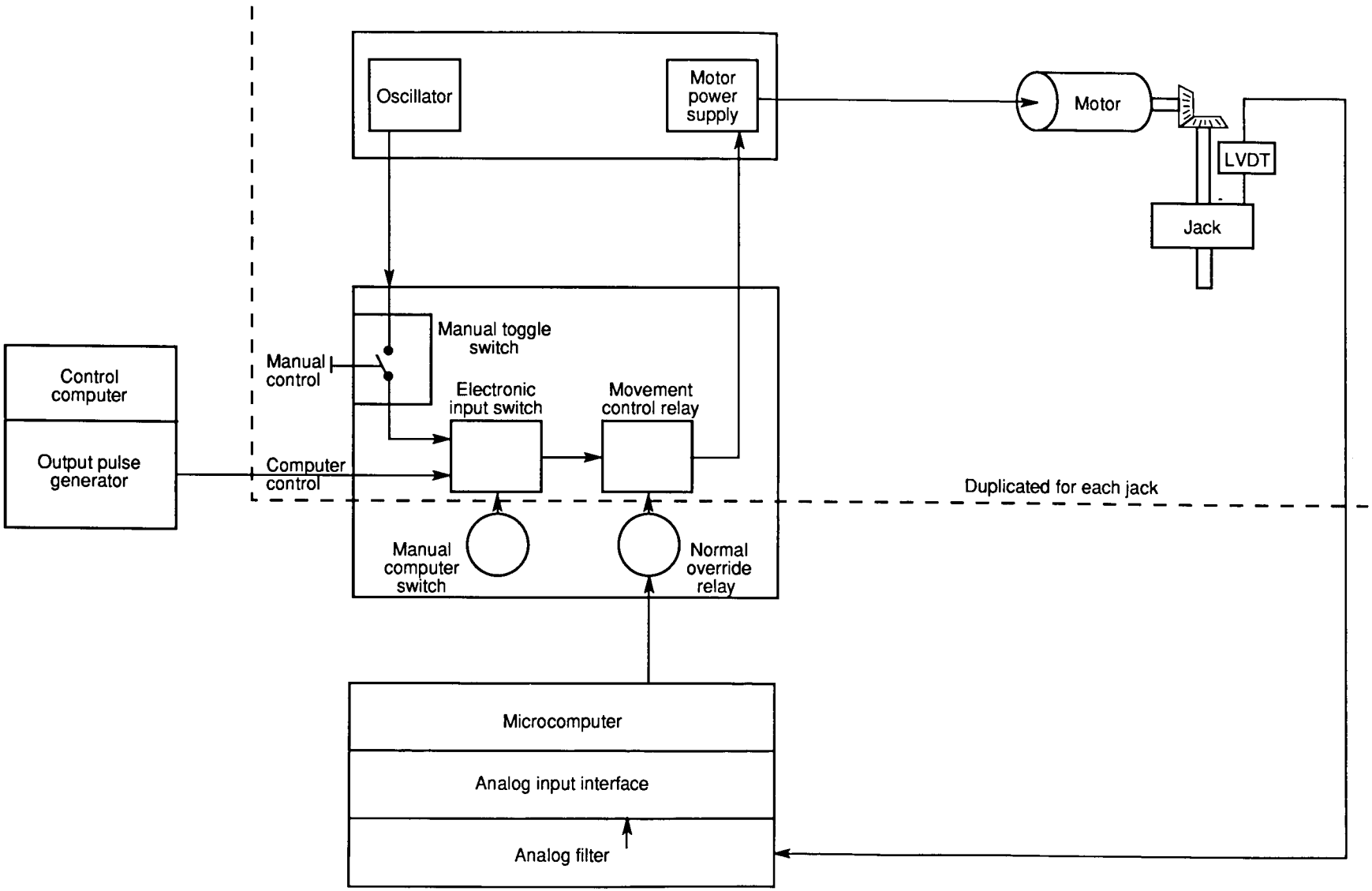

Figure 21. Operational diagram of wall movement and wall protection system.

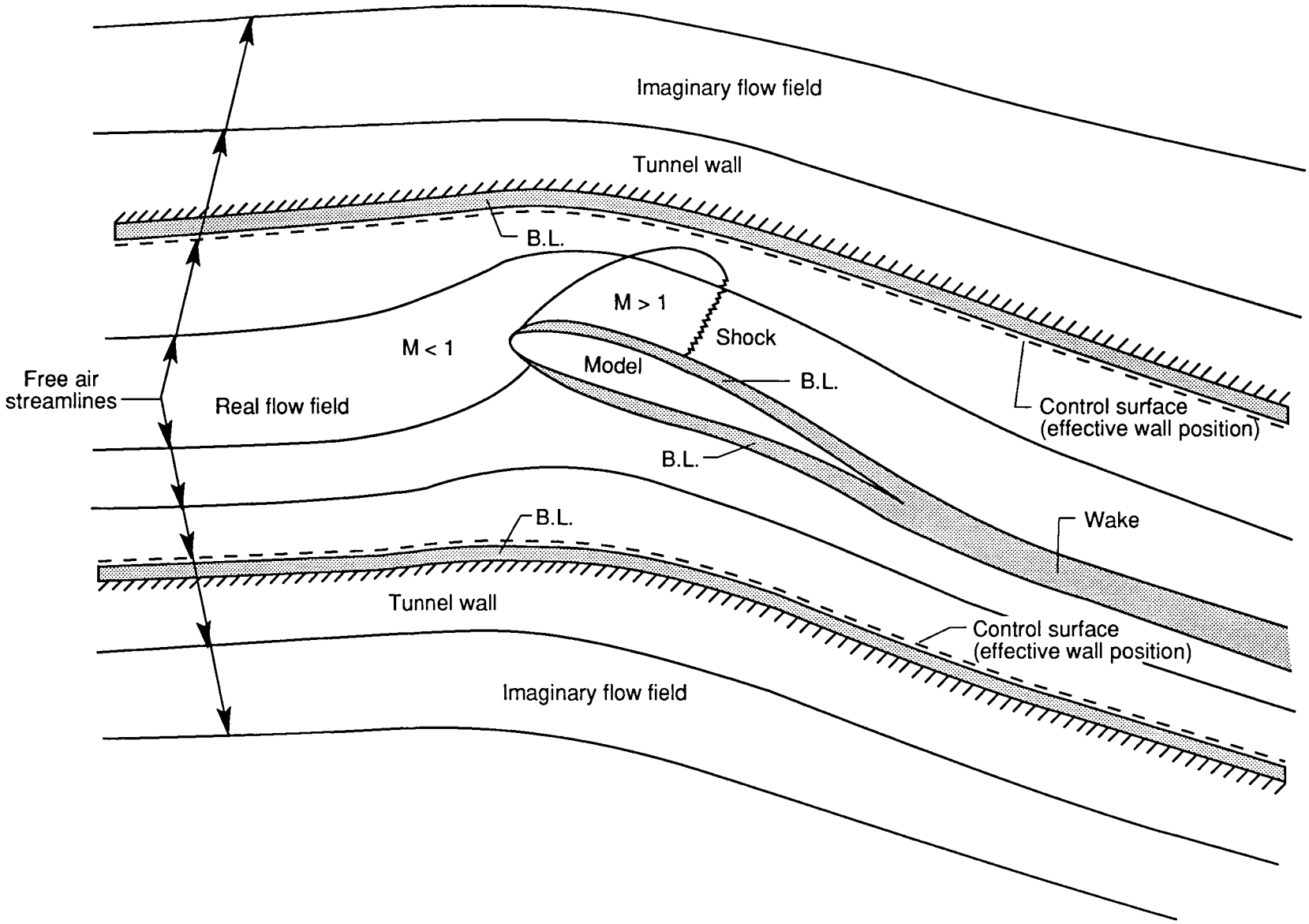

Figure 22. Assumed flow field for adaptive wall test section.

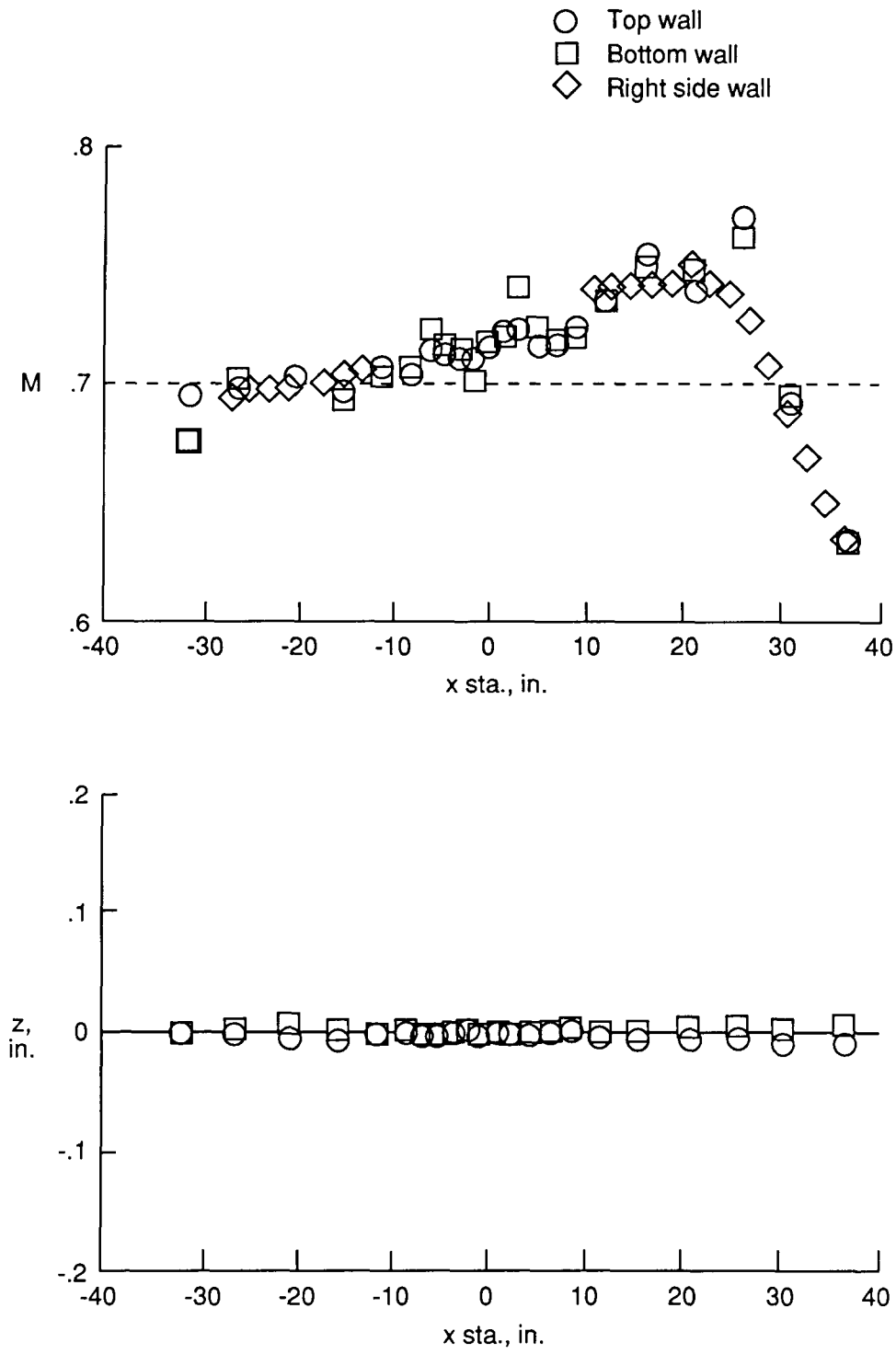

(a) Undeflected walls.

Figure 23. Test section Mach number distribution for several wall shapes.

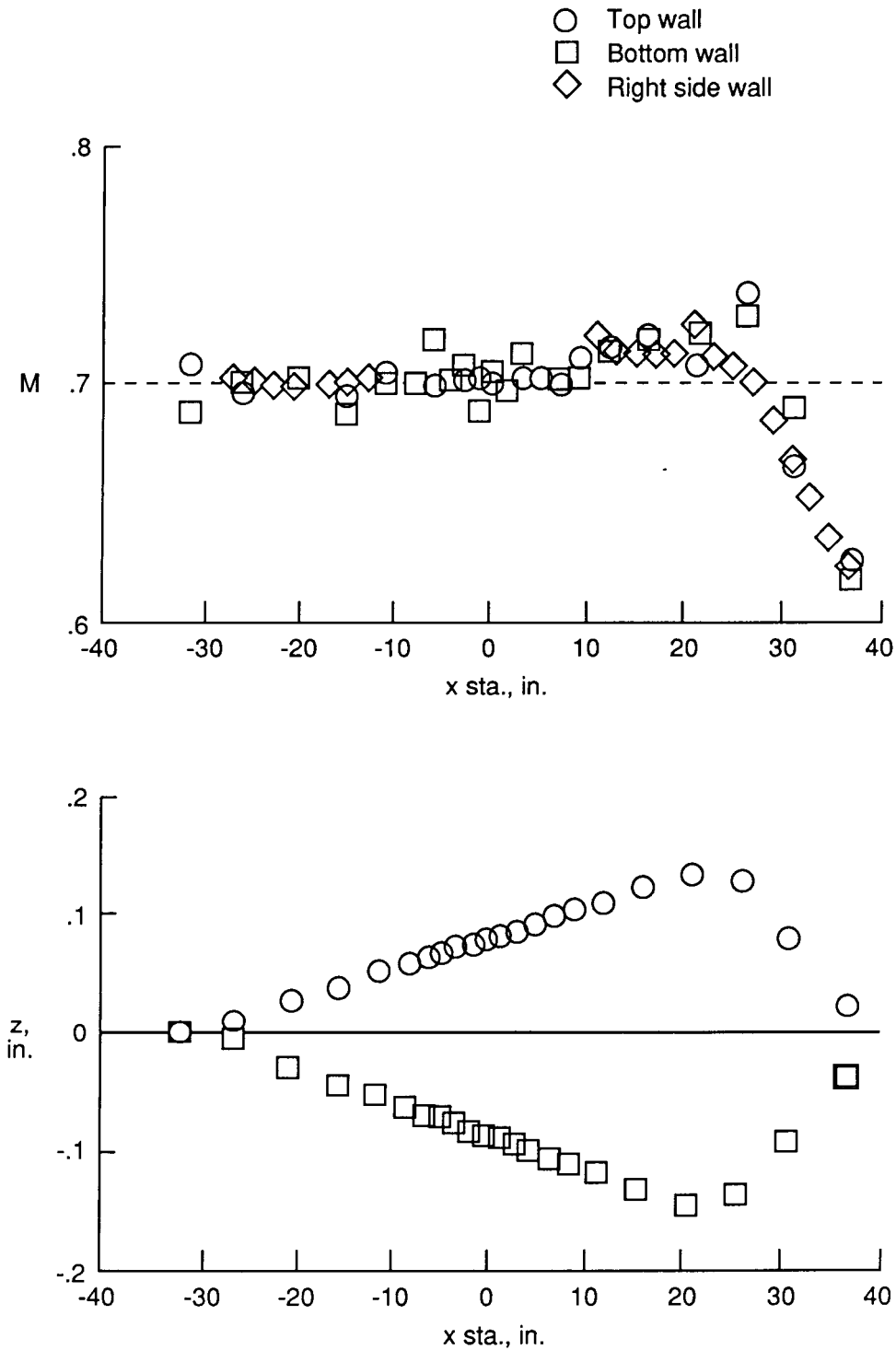

(b) Linearly diverged walls.

Figure 23. Continued.

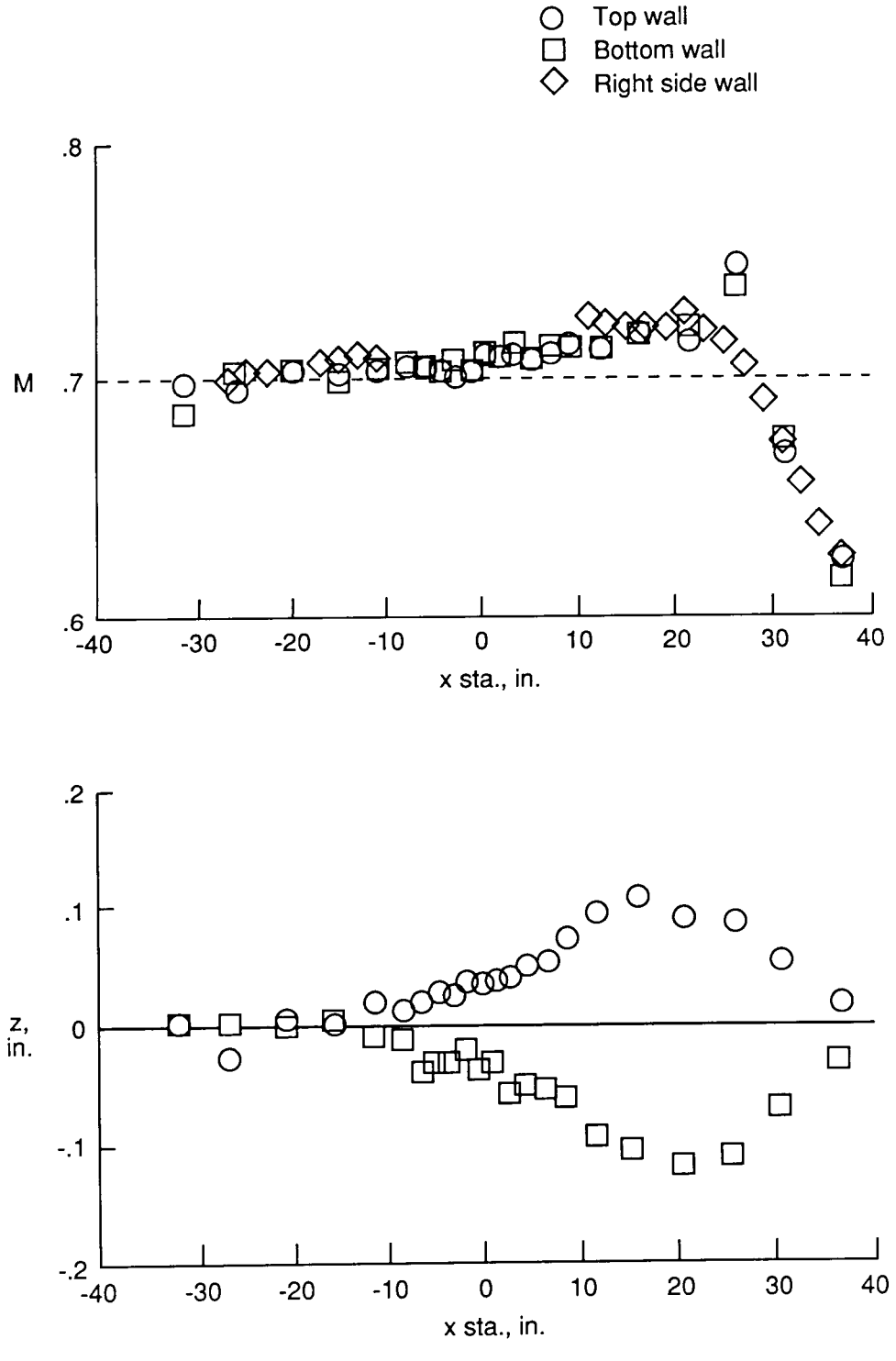

(c) Partially adapted walls.

Figure 23. Concluded.

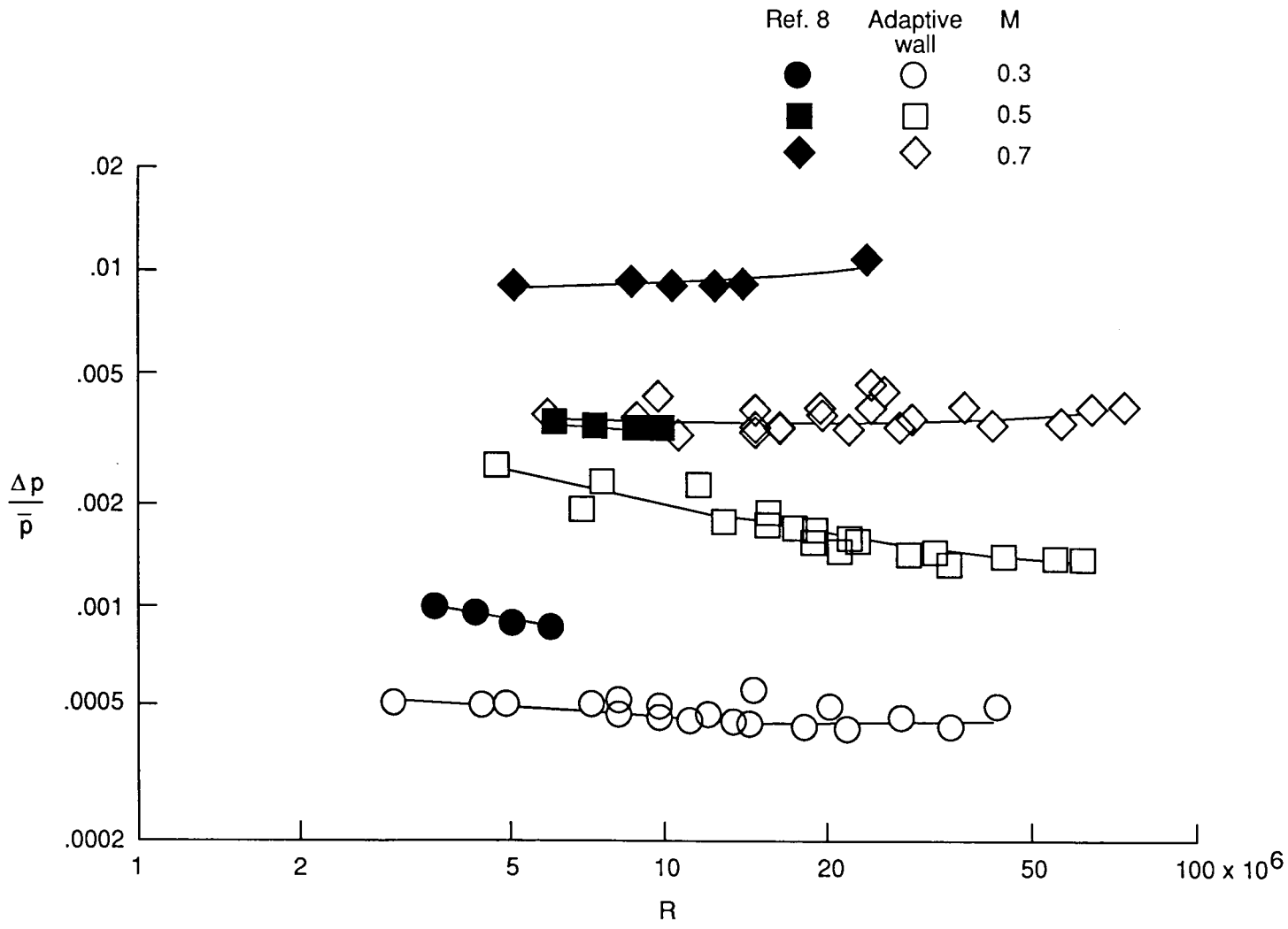

Figure 24. Comparison of sidewall fluctuating pressures in slotted test section (ref. 8) and adaptive wall test section.

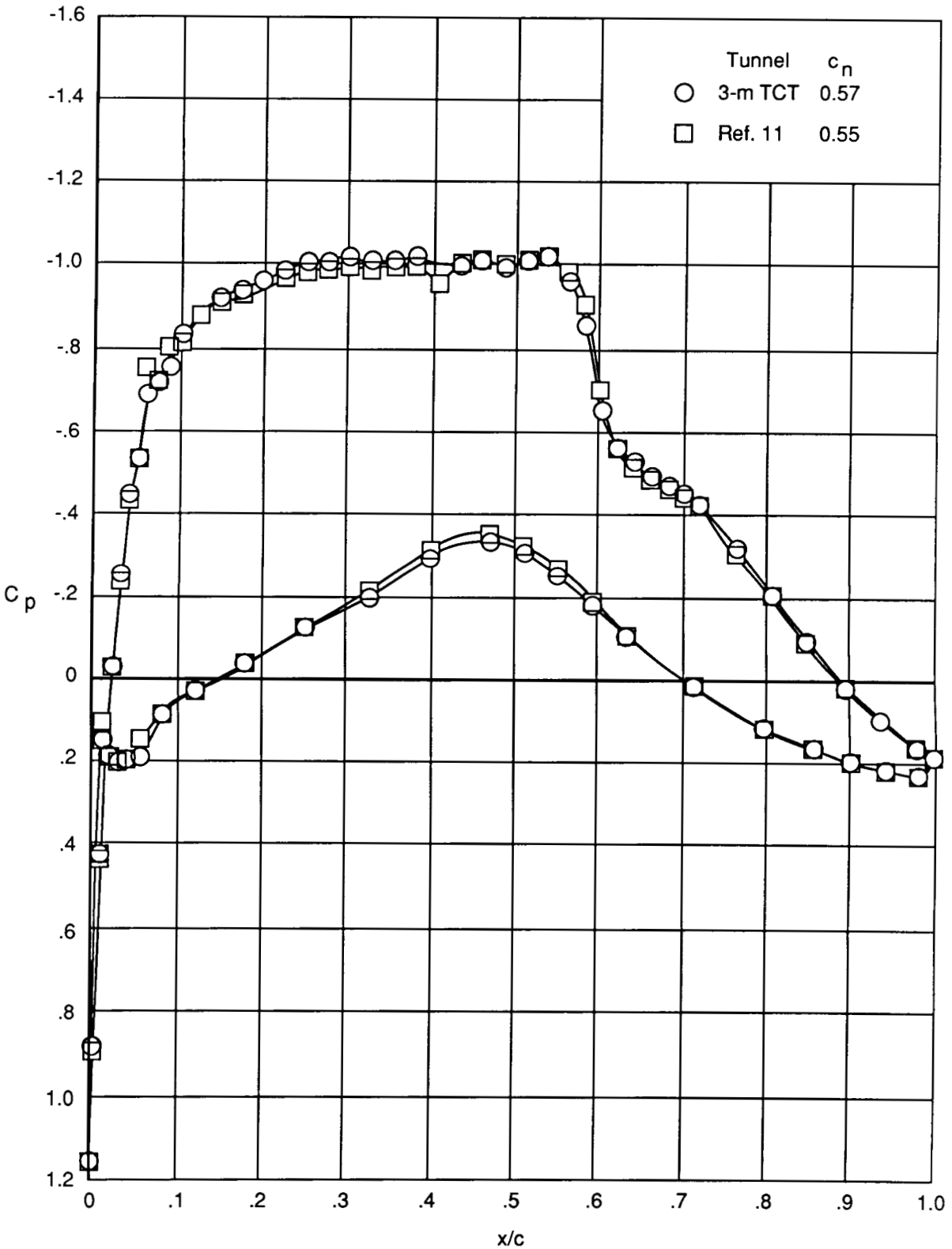

(a) Chordwise pressure distribution.

Figure 25. Sample of model pressures and test section boundary conditions. $M = 0.765$.

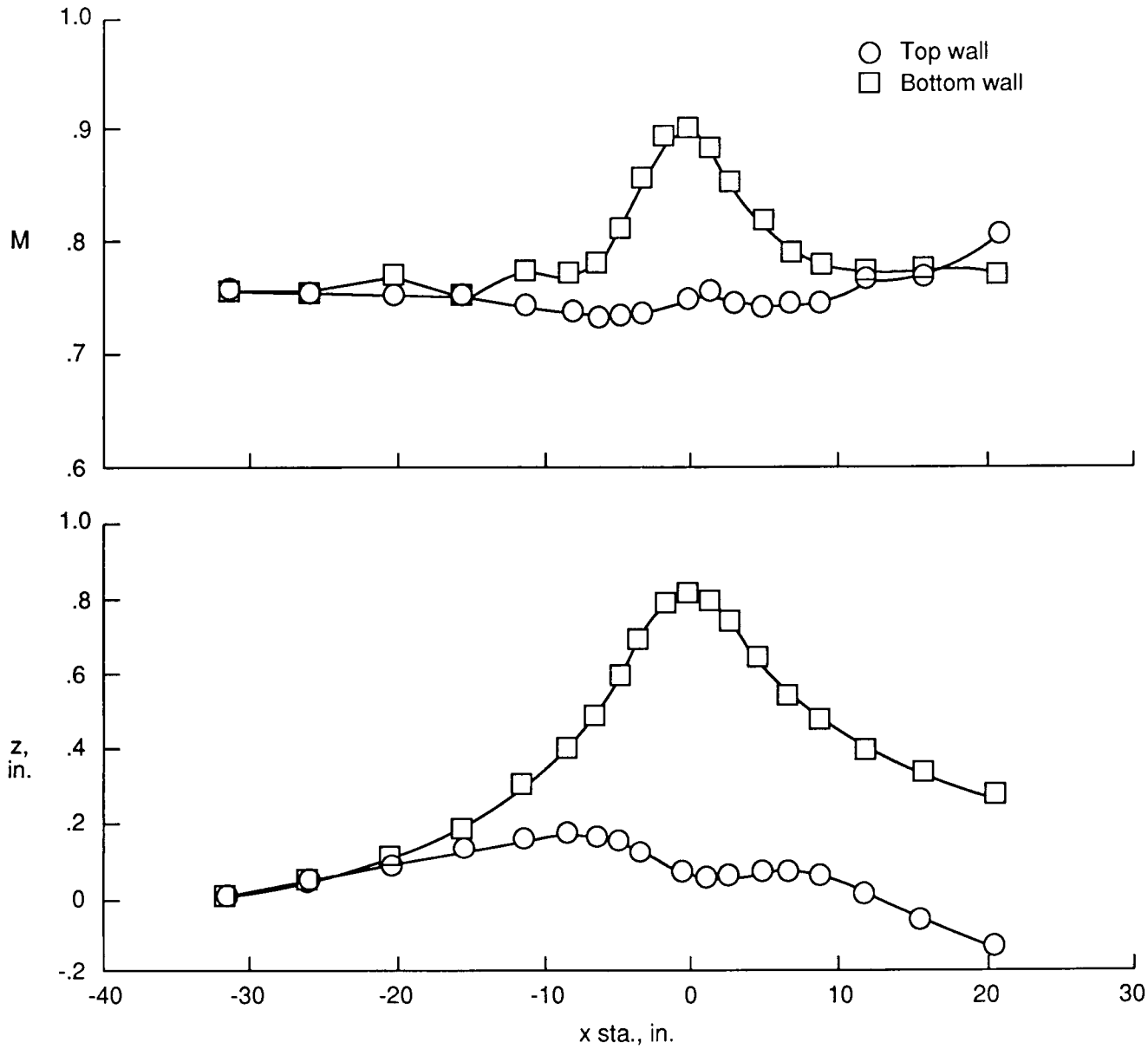

(b) Test section boundary conditions.

Figure 25. Concluded.

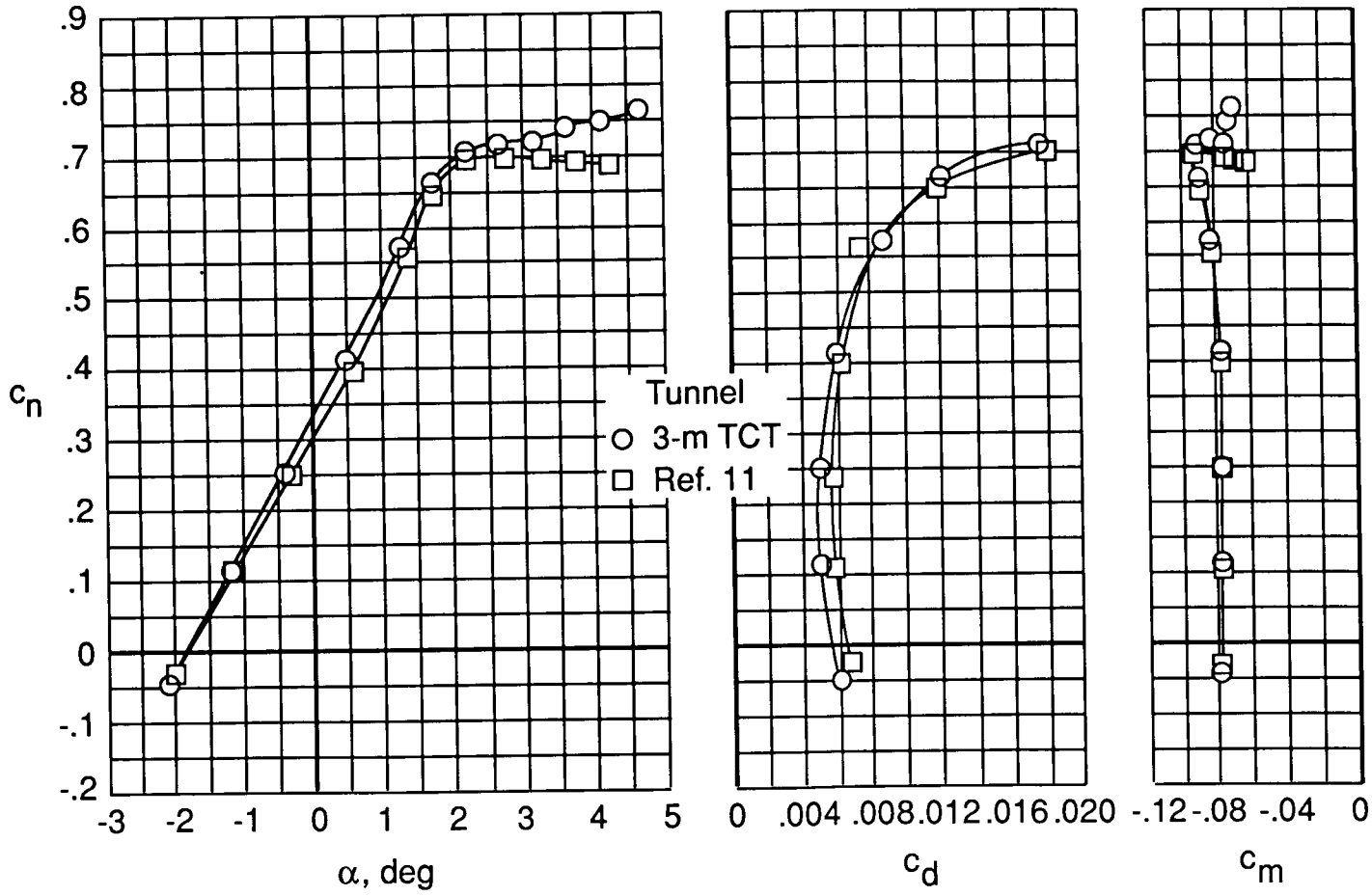

Figure 26. Comparison of integrated force and moment coefficients. $M = 0.765$.

NASA
National Aeronautics and Space Administration

Report Documentation Page

1. Report No.	2. Government Accession No.	3. Recipient's Catalog No.
NASA TM-4114		

4. Title and Subtitle	5. Report Date
Hardware and Operating Features of the Adaptive Wall Test Section for the Langley 0.3-Meter Transonic Cryogenic Tunnel	June 1989
	6. Performing Organization Code
7. Author(s)	8. Performing Organization Report No.
Raymond E. Mineck	L-16548
9. Performing Organization Name and Address	10. Work Unit No.
NASA Langley Research Center Hampton, VA 23665-5225	505-61-21-03
	11. Contract or Grant No.
12. Sponsoring Agency Name and Address	13. Type of Report and Period Covered
National Aeronautics and Space Administration Washington, DC 20546-0001	Technical Memorandum
	14. Sponsoring Agency Code

15. Supplementary Notes

16. Abstract

A 13- by 13-inch adaptive wall test section has been installed in the Langley 0.3-Meter Transonic Cryogenic Tunnel circuit. This new test section has four solid walls and is configured for two-dimensional airfoil testing. The top and bottom walls are flexible and movable, whereas the sidewalls are rigid and fixed. The test section has a turntable to support airfoil models, a survey mechanism to probe the model wake, and provisions for a sidewall boundary-layer-control system. Details of the adaptive wall test section, the tunnel circuit modifications, the supporting instrumentation, the monitoring and control hardware, and the wall adaptation strategy are discussed. Sample results of shakedown tests with the test section empty and with an airfoil installed are also included.

17. Key Words (Suggested by Authors(s))	18. Distribution Statement
Cryogenic tunnels Two-dimensional test sections Adaptive wall test sections	Unclassified—Unlimited Subject Category 09

19. Security Classif. (of this report)	20. Security Classif. (of this page)	21. No. of Pages	22. Price
Unclassified	Unclassified	39	A03

NASA-Langley, 1989

For sale by the National Technical Information Service, Springfield, Virginia 22161-2171